IMPROVING ADVANCED BIOFUELS PRODUCTION IN *SACCHAROMYCES CEREVISIAE* VIA PROTEIN ENGINEERING AND SYNTHETIC BIOLOGY APPROACHES

BY

JIAZHANG LIAN

THESIS

Submitted in partial fulfillment of the requirements
for the degree of Master of Science in Chemical Engineering
in the Graduate College of the
University of Illinois at Urbana-Champaign, 2013

Urbana, Illinois

Adviser:

Professor Huimin Zhao

Abstract

Saccharomyces cerevisiae has been widely established as a platform microorganism for industrial production of fuels and chemicals from lignocellulosic biomass. However, we are still encountering several challenges to achieve cost-effective production of cellulosic biofuels, such as the sequential utilization of sugar mixtures caused by glucose repression and the low efficiency of synthesizing fatty acid derived advanced biofuels.

In this thesis, we aim to improve the production of advanced biofuels in *S. cerevisiae* using protein engineering and synthetic biology approaches. To overcome glucose repression, a cellobiose utilization pathway consisting of a cellodextrin transporter and a β-glucosidase was introduced into *S. cerevisiae* to allow co-fermentation of mixed sugars. However, the utilization of cellobiose was still much lower than that of glucose, and the uptake of cellobiose was considered the rate-limiting step for cellobiose fermentation. Therefore, directed evolution of the cellodextrin transporter (CDT2) was carried out to improve the uptake activity and thus cellobiose fermentation. After three rounds of directed evolution, both the specific activity and transporter expression level of CDT2 were increased, leading to 2.15 fold improvement of the cellobiose uptake activity. Using high cell density fermentation under anaerobic conditions, the best mutant conferred 2.67 fold and 4.96 fold increase in the cellobiose consumption rate and ethanol productivity, respectively.

Besides bioethanol, we are also interested in advanced biofuels that have similar properties to current transportation fuels. Since most of the advanced biofuels are derived from fatty acids, efficient production is limited by the low efficiency and high energy input of the fatty acid biosynthesis pathways. Reversal of β-oxidation cycles has been engineered to produce a

series of fatty acid derived fuels and chemicals in *Escherichia coli*. Thus, another goal of this thesis is to construct a new fatty acid biosynthesis platform based on the reversal of β-oxidation cycles for advanced biofuel production in *S. cerevisiae*. Using synthetic biology approaches, reversed β-oxidation pathways were constructed and characterized to be able to produce butanol, indicating the functional reversal of β-oxidation cycles. Future work will focus on expanding this platform to produce other fatty acid derived advanced biofuels such as biodiesel (fatty acid ethyl ester, FAEE).

To my wife, family, and friends

Acknowledgement

First and foremost, I would like to thank my advisor Huimin Zhao for his guidance on these projects. He not only trained my experimental skills, but also the essence to be a good researcher. He is also acknowledged for persuading me to join the University of Illinois at Urbana-Champaign and his group to start my academic life and his continuous help in preparing for my future career.

I am also very thankful to all Zhao Group members for their helpful discussions, friendship, and assistance, especially Yongbo Yuan, Sijin Li, Ran Chao, Tong Si, Dan Coursolle, Dawn Eriksen, Meng Wang, and Xueyang Feng to work together as a team in the Energy Biosciences Institute. I would like to thank Mohammad (Sam) Hamedi Rad for his help in the CDT2 engineering project, and Ran Chao and Zehua Bao for their help in cloning FOX2 homologs from different yeast species for the reversed β-oxidation project. I also would like to thank Dr. Mayandi Sivaguru from the Core Facilities at the Institute for Genomic Biology at the University of Illinois at Urbana-Champaign for his help with the confocal microscopy.

Finally, I would like to express my most sincere gratitude to my wife Jiewen Zhou, my parents, and my friends for their constant support. In addition, I would like to give special thanks to our baby who will come soon in a couple of months to bring us surprise and happiness.

Table of Contents

Chapter 1 Introduction

1.1 Cellulosic Biofuels

Biological conversion of plant-derived lignocellulosic materials into biofuels has been intensively investigated as a result of increasing concerns on energy security, sustainability and global climate change (1). *Saccharomyces cerevisiae*, also known as baker's yeast, which has been used for alcohol fermentation for thousands of years, is an excellent organism for cellulosic biofuel production, for its high tolerance to alcohols, well-studied genetic and physiological background, the availability of large number of genetic tools, and the compatibility of high-density and large-scale fermentation (2). Unfortunately, wild type *S. cerevisiae* strains cannot utilize pentose sugars, especially xylose, the second most abundant carbohydrate component in lignocellulosic biomass. Heterologous xylose utilization pathways, including the bacterial isomerase pathway and the fungal oxo-reductive pathway, have been introduced to enable xylose metabolism (3). Although steady progress has been achieved to construct efficient xylose-fermenting yeasts after intensive engineering work, the uptake and metabolism of xylose are still completely inhibited by glucose (4-6). One explanation for glucose repression (or catabolite repression) lies in the lack of xylose specific transporters in *S. cerevisiae*. Thus, xylose can only be transported via the hexose transporters, whose affinity for xylose is two orders of magnitude lower than that for glucose (7-9). This glucose repression phenomenon results in sequential utilization of glucose and xylose (Figure 1.1A), thus low yield and productivity of biofuels (4). Therefore, the construction of a yeast strain that can consume sugar mixtures efficiently and simultaneously is one of the biggest challenges for cost-effective production of cellulosic biofuels.

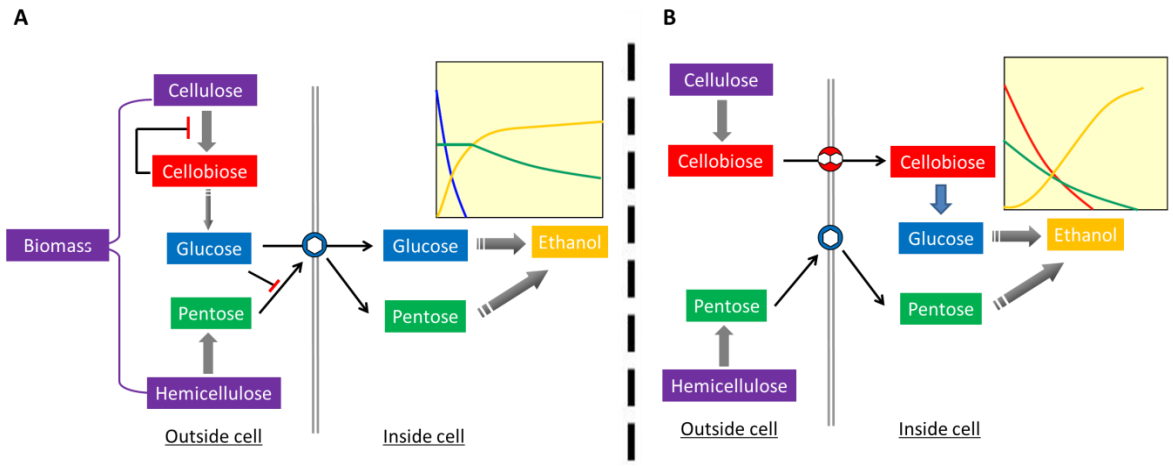

Figure 1.1 Introduction of a cellodextrin transporter and an intracellular β-glucosidase allowing cellobiose/xylose co-fermentation. The traditional biofuel production scheme (A) suffers from sequential sugar utilization and low production efficiency, while the cellobiose fermentation strategy (B) allows simultaneous utilization of mixed sugars, thus higher biofuel production efficiency. Red, blue, green, and yellow color indicates cellobiose, glucose, pentose, and ethanol, respectively.

Recently, cellodextrin transporters were identified and characterized, and co-expression of a cellodextrin transporter and an intra-cellular β-glucosidase was proposed to be an efficient strategy to eliminate glucose repression in *S. cerevisiae* (10). In this system, cellobiose is transported by the cellodextrin transporter and hydrolyzed by β-glucosidase to release glucose intracellularly. Since the intracellularly released glucose is metabolized very fast, there will be no or very low glucose present in the medium, which liberates the hexose transporters for pentose uptake only. In other word, cellobiose and pentose can enter the cell via two separate transportation systems. As a result, glucose repression was eliminated and co-fermentation of cellobiose/xylose (5, 6) and cellobiose/galactose (11) were achieved in the engineered yeast strain (Figure 1.1B).

Currently, two cellodextrin transporters were characterized from *Neurospora crassa*: cellodextrin transporter 1 (CDT1) is a symporter with higher cellobiose uptake activity (V_{max}),

while cellodextrin transporter 2 (CDT2) is a facilitator with much lower activity (10). Recent work on improving cellobiose fermentation performance mainly focused on CDT1 (5, 6, 11-16), because of the higher transporter activity and better cellobiose fermentation performance under aerobic or oxygen-limited conditions. However, CDT1 is not optimal for anaerobic fermentation, a preferred process for industrial applications, since energy (ATP) consumption is coupled to cellobiose uptake. On the contrary, the facilitator nature of CDT2 endows the energetic benefits under anaerobic conditions, due to no ATP consumption for cellobiose uptake. Therefore, CDT2 has the potential to develop a better system for industrial production of cellulosic biofuels.

1.2 Directed Evolution of Transporters

Protein engineering, including the directed evolution approach, the knowledge-driven rational design approach, and a hybrid approach combining directed evolution and rational design, has been widely used to improve the performance of a wide variety of enzymes and pathways (17, 18). Although directed evolution has been successfully used to improve the activity, specificity, and stability of industrially important enzymes (19-21), its utilization in membrane-bound protein engineering is only limited to a few applications, such as the light-transducing protein bacteriorhodopsin (22, 23), bacterial efflux pumps (24, 25), and xylose transporters in both *Escherichia coli* (26) and *S. cerevisiae* (27). The membrane-bound feature of these proteins significantly limits the power of protein engineering. Rational design is hindered by the lack or limited availability of high-resolution structural information. Due to the difficulties in expressing and crystalizing membrane proteins, there are only a few crystal structures available, especially for transporter proteins (28, 29). To date (as of May 31, 2013), there are only 1,271 membrane proteins with crystal structures (http://blanco.biomol.uci.edu/mpstruc/), whereas there are 91,359

structures deposited into the Protein Data Bank (http://www.rcsb.org/pdb/home/home.do). Directed evolution is limited by the difficulty in determining the activity of membrane proteins, let alone the development of a high-throughput screening system. As the bridge between intra- and extra-cellular environment, membrane proteins are mainly involved in the transduction of extracellular signals, transportation of substances through membrane, and generation of energy, whose activities are difficult or labor-intensive to determine (30, 31). Fortunately, sugar transporters, mediating the uptake of sugars into cells, are essential to initiate the cellular metabolism, and a high throughput screening method based on cell growth rate can be readily developed. Engineering of xylose transporters was carried out in a host with the xylose utilization pathway integrated to the chromosome and all hexose transporters inactivated (27). Due to the lack of an endogenous cellobiose uptake system in *S. cerevisiae*, it will be much easier and straightforward to develop a high throughput screening method, such as the colony size based screening strategy for cellodextrin transporter engineering.

1.3 Fatty Acid Derived Advanced Biofuels

Although ethanol is currently the leading biofuel molecule produced as the alternative transportation fuel, it has many shortcomings such as low energy density, high corrosivity, and hydroscopicity (32). Thus, there is an increasing effort to produce advanced biofuels or the so-called “drop-in” biofuels that have similar properties to current transportation fuels. Examples of advanced biofuels include butanol, fatty acid ethyl ester (FAEE), and alkane, all of which can be produced from either the natural or engineered fatty acid biosynthetic pathways (33).

Fatty acid biosynthesis (FAB) is catalyzed by the enzyme system called fatty acid synthase (FAS), which is rather conserved in nature. The classic FAB involves in the elongation of acyl-acyl carrier protein (ACP) precursors using malonyl-ACP as the extender unit (34). The generated long chain fatty acyl-ACPs can be converted to alkanes by introducing a heterologous pathway from cyanobacteria containing an acyl-ACP reductase (AAR) and an aldehyde deformylating oxygenase (ADO) (35). As for the production of biodiesels (FAEEs) and fatty alcohols (36, 37), fatty acyl-CoAs are the substrate, which can also be generated from fatty acyl-ACPs. Free fatty acids are released from the ACP group by thioesterase (TE) and then activated to form fatty acyl-CoAs by fatty acyl-CoA synthase (FAA). The synthesis of FAEEs and fatty alcohols are catalyzed by wax synthase/diacylglycerol acyltransferase (WS/DGAT) and fatty acyl-CoA reductase (FAR), respectively (Figure 1.2).

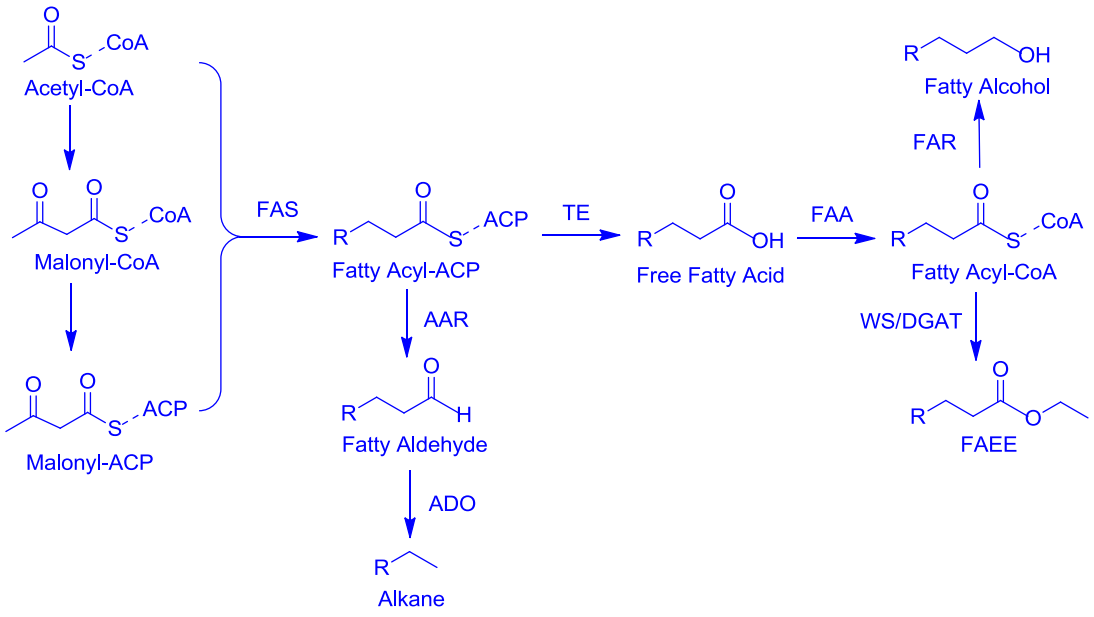

Figure 1.2 Overview of the production of fatty acid derived advanced biofuels. FAS, fatty acid synthase; AAR, acyl-ACP reductase; ADO, aldehyde deformylating oxygenase; TE, thioesterase; FAA, fatty acyl-CoA synthase; FAR, fatty acyl-CoA reductase; WS/DGAT, wax synthase/diacylglycerol acyltransferase.

Although the significance of FAB in advanced biofuels production, fatty acid does not accumulate to high levels naturally, due to the low flux and high regulation. Therefore, intensive metabolic engineering work has been carried out to re-direct the flux to FAB, such as the overexpression of thioesterase, fatty acyl-CoA synthase, acetyl-CoA carboxylase, and global transcription factors (38). Besides the classic FAB mechanisms shared by most of organisms, nature also evolved several special mechanisms to synthesize fatty acids *de novo*, such as the elongase system (39, 40) and fermentative pathway (41, 42). Although not widely distributed in nature, these special pathways possess significant advantages over the traditional ones, in terms of pathway efficiency and controllability of the fatty acid chain length.

1.3.1 Traditional Type-I and Type-II FAS

Based on the architecture, FAS can be divided into two classes, type-I FAS and type-II FAS, which are mainly present in eukaryotes and prokaryotes, respectively (43). The type-I FAS is characterized by being composed of large multifunctional polypeptides that carry all the proteins necessary for FAB on one or two large polypeptide chains. In the case of type-II system, mono-functional proteins are discretely expressed from a series of separate genes. Type-II FAS is found mostly in bacteria, but also in eukaryotic organelles, such as mitochondria and plastids (34). In some actinomycetes, such as *Mycobacterium* species, both type-I and type-II FASs are present (44).

Although the organization of the FAS system varies between different organisms, the individual enzymatic reactions of FAB are essentially the same (34, 43). FAB begins with the conversion of acetyl-CoA into malonyl-CoA by acetyl-CoA carboxylase (ACC) at the cost of

ATP, which is then transferred to ACP by malonyl-CoA:ACP transacylase. The generated malonyl-ACP is used as an extender unit, condensing with acyl-ACP to form β-ketoacyl-ACP with two more carbon units. The extended β-ketoacyl-ACP is subject to an NADPH-dependent reduction to form β-hydroxyacyl-ACP, whose hydroxyl group is removed by β-hydroxyacyl-ACP dehydratase, leading to the formation of *trans*-2-enoyl-ACP. The double bond is then reduced in another NADPH-dependent reaction by the *trans*-2-enoyl-ACP reductase. Each elongation cycle results in the synthesis of acyl-ACP with the fatty acyl chain extended by two carbon units.

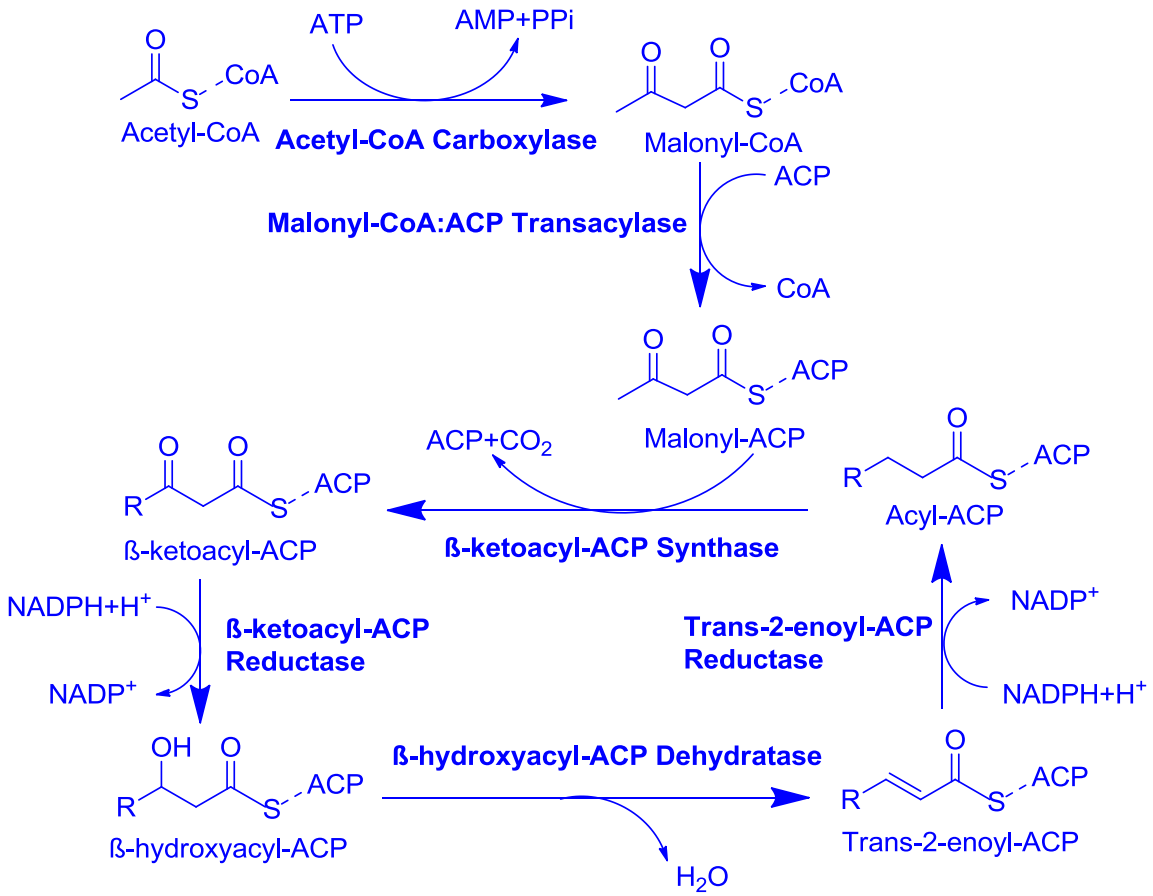

Figure 1.3 Overview of the traditional FAB mechanisms. The elongation cycle is repeated several times, until the generation of C_{16}- or C_{18}-ACP.

1.3.2 Elongase for de novo Fatty Acid Biosynthesis

As mentioned above, the traditional FAS system utilizes malonyl-ACP as the extender unit and NADPH as the reducing force to elongate the acyl chain, highlighting the ATP, NADPH, and ACP dependence (34). A different *de novo* FAS system, the microsomal elongase, was described in *Trypanosoma brucei*, a eukaryotic human parasite that causes sleeping sickness (39, 40). Genome sequence indicates the presence of a putative Type-II FAS system, but experimental results suggest that Type-II FAS is not responsible for *de novo* fatty acid synthesis. 1) The components are membrane associated proteins, while soluble proteins are generally found for a Type-II FAS system. 2) Several traditional Type-II FAS inhibitors, such as triclosan and cerulenin, which inhibit *trans*-2-enoyl-ACP reductase and β-ketoacyl-ACP synthase (45), respectively, will not affect the bulk fatty acid synthesis. 3) RNA interference (RNAi) silencing of ACP, a key component of type II systems, has no effect on *de novo* FA synthesis as well. Later, the system was characterized to use three elongases instead of a type-II synthase (Figure 1.4).

In this microsomal elongase system, malonyl-CoA serves as the extender unit and CoA is the acyl chain carrier. In other words, this system is ATP, NADPH, and CoA dependent. What's more, trypanosomes have different fatty acid requirements during their life cycle, as they encounter various growth environments (39). It is found that the fatty acid requirement was achieved via the chain specificity of elongases, with Elo1 converting C_4 to C_{10}-CoA, Elo2 extending C_{10} to C_{14}-CoA, and Elo3 elongating C_{14} to C_{18}-CoA (Figure 1.4). The modular property of the elongase system will allow the accessibility for chain length engineering. For example, if only Elo1 is included into the cyanobacterial alkane biosynthetic pathway, C_7 and C_9 alkanes will be the major products, which are the same as gasoline.

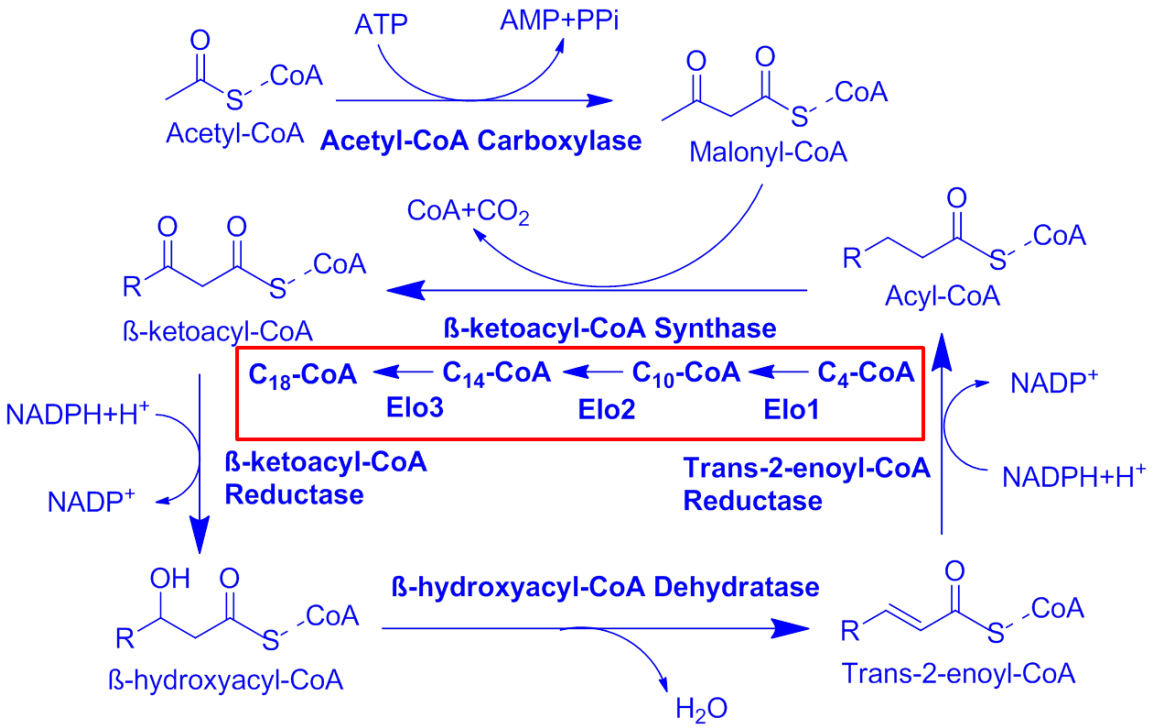

Figure 1.4 Trypanosomal elongase system for *de novo* fatty acid biosynthesis.

1.3.3 Fermentative Fatty Acid Biosynthesis in the Mitochondria of Euglena gracilis

Another special mechanism for *de novo* FAB was described in the mitochondria of *Euglena gracilis (41, 42)*. So far, five different FAS systems have been reported for *E. gracilis*, two type-II FAS localized in the chloroplasts, one type-I FAS in the cytosol, one microsomal FAS, and one mitochondrial FAS. The mitochondrial system is involved in anaerobic wax ester fermentation. This fermentative system was featured to be malonyl-CoA (or ATP) independent, and have the ability to synthesize fatty acids directly from acetyl-CoA as both primer and extender. In addition, NADH, instead of NADPH, serves as the reducing power (Figure 1.5). Due to the ATP and ACP independence and CoA and NADH dependence, the fermentative FAB proceeds by reversal of the β-oxidation cycles. Compared with the traditional FAB, the fermentative pathway is featured for its energetic benefits of ATP independence and availability

of CoA and NADH versus ACP and NADPH inside the cell. The advantages of such system was demonstrated by a recent report to reverse β-oxidation cycles to synthesize a series of chemicals and fuels at the highest titer ever reported (46, 47). Although genes coding the fermentative fatty acid synthesis pathway are not well characterized yet, the availability of its genome sequence will definitely help to decipher the genetic code and benefit in designing efficient fatty acid derived biofuel synthetic pathways.

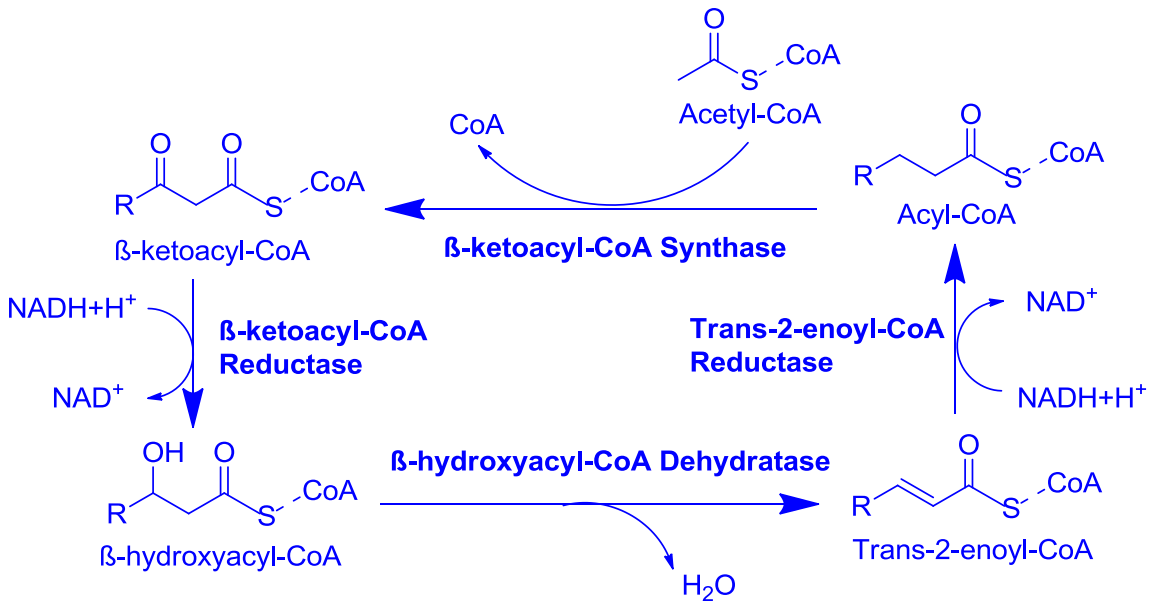

Figure 1.5 Fermentative fatty acid biosynthesis in the mitochondrion of *Euglena gracilis*.

1.4 Project Overview

This thesis focuses on improving advanced biofuels production in *S. cerevisiae* using protein engineering and synthetic biology approaches. One of the major challenges for economical biofuel production is to consume all sugar components efficiently and simultaneously, due to the widely distribution of glucose repression in nature. Although cellobiose fermentation has been set as an efficient system to achieve mix sugar co-fermentation, its utilization rate is still much lower than that of glucose. Thus, one aim of this thesis is to improve the efficiency of cellobiose

fermentation via directed evolution of the cellodextrin transporter, which is considered as rate-limiting for cellobiose metabolism. Besides bioethanol, increasing effort in biofuel industry is devoted to producing advanced biofuels that have similar properties to current transportation fuels. Currently, efficient advanced biofuel production is limited by the low flux, high energy input, and complicated regulation of FAB. Thus, another aim of this thesis is to construct a new FAB platform for advanced biofuel production. Notably, aim 1 and aim 2 can be integrated to allow the production of advanced biofuels from cellulosic materials, which is the ultimate goal of bioenergy research.

Chapter 2 mainly focused on improving anaerobic cellobiose fermentation via directed evolution of the cellodextrin transporter. As mentioned, CDT1 is a symporter with higher cellobiose uptake activity (V_{max}), while CDT2 is a facilitator with much lower activity. Although CDT2 has the potential to develop a better system for industrial production of cellulosic biofuels due to the energetic benefits of no ATP consumption for cellobiose uptake, cellobiose fermentation is limited by the low transporter activity. To overcome the main limitation of CDT2, we sought to increase its cellobiose uptake activity using a directed evolution strategy.

In Chapter 3 of this thesis, we attempted to reverse β-oxidation cycles in yeast for efficient production of advanced biofuels. Compared with the traditional FAB, which is ATP, ACP, and NADPH dependent, the reversed β-oxidation pathway is featured for its ATP and ACP independence and CoA and NADH dependence. The energetic benefits of ATP independence and availability of CoA and NADH versus ACP and NADPH confer advantages for efficient fatty acid biosynthesis. Recent reports to synthesize a series of chemicals and fuels were achieved by reversing β-oxidation cycles in *Escherichia coli* via systems biology and synthetic biology approaches. The advantages of such system was demonstrated by the highest reported

titers of fuels and chemicals produced. Taking the merits of yeast for biofuel production into account, we sought to develop a platform for advanced biofuel production based on the reversal of β-oxidation cycles via synthetic biology approaches in *S. cerevisiae*.

1.5 References

1. **Du J, Shao Z, Zhao H.** 2011. Engineering microbial factories for synthesis of value-added products. J. Ind. Microbiol. Biotechnol. **38:**873-890.
2. **Hong KK, Nielsen J.** 2012. Metabolic engineering of *Saccharomyces cerevisiae*: a key cell factory platform for future biorefineries. Cell Mol. Life Sci. **69:**2671-2690.
3. **Hahn-Hagerdal B, Karhumaa K, Jeppsson M, Gorwa-Grauslund MF.** 2007. Metabolic engineering for pentose utilization in *Saccharomyces cerevisiae*. Adv. Biochem. Eng. Biotechnol. **108:**147-177.
4. **Kim SR, Ha SJ, Wei N, Oh EJ, Jin YS.** 2012. Simultaneous co-fermentation of mixed sugars: a promising strategy for producing cellulosic ethanol. Trends Biotechnol. **30:**274-282.
5. **Li S, Du J, Sun J, Galazka JM, Glass NL, Cate JH, Yang X, Zhao H.** 2010. Overcoming glucose repression in mixed sugar fermentation by co-expressing a cellobiose transporter and a beta-glucosidase in Saccharomyces cerevisiae. Mol. Biosyst. **6:**2129-2132.
6. **Ha SJ, Galazka JM, Kim SR, Choi JH, Yang X, Seo JH, Glass NL, Cate JH, Jin YS.** 2011. Engineered *Saccharomyces cerevisiae* capable of simultaneous cellobiose and xylose fermentation. Proc. Natl. Acad. Sci. U. S. A. **108:**504-509.
7. **Jojima T, Omumasaba CA, Inui M, Yukawa H.** 2010. Sugar transporters in efficient utilization of mixed sugar substrates: current knowledge and outlook. Appl. Microbiol. Biotechnol. **85:**471-480.
8. **Sedlak M, Ho NW.** 2004. Characterization of the effectiveness of hexose transporters for transporting xylose during glucose and xylose co-fermentation by a recombinant *Saccharomyces* yeast. Yeast **21:**671-684.
9. **Du J, Li S, Zhao H.** 2010. Discovery and characterization of novel D-xylose-specific transporters from *Neurospora crassa* and *Pichia stipitis*. Mol. Biosyst. **6:**2150-2156.
10. **Galazka JM, Tian C, Beeson WT, Martinez B, Glass NL, Cate JH.** 2010. Cellodextrin transport in yeast for improved biofuel production. Science **330:**84-86.
11. **Ha SJ, Wei Q, Kim SR, Galazka JM, Cate JH, Jin YS.** 2011. Cofermentation of cellobiose and galactose by an engineered *Saccharomyces cerevisiae* strain. Appl. Environ. Microbiol. **77:**5822-5825.
12. **Ha SJ, Galazka JM, Oh EJ, Kordic V, Kim H, Jin YS, Cate JH.** 2013. Energetic benefits and rapid cellobiose fermentation by *Saccharomyces cerevisiae* expressing cellobiose phosphorylase and mutant cellodextrin transporters. Metab. Eng. **15:**134-143.

13. **Oh EJ, Ha SJ, Kim SR, Lee WH, Galazka JM, Cate JH, Jin YS.** 2013. Enhanced xylitol production through simultaneous co-utilization of cellobiose and xylose by engineered *Saccharomyces cerevisiae*. Metab. Eng. **15:**226-234.
14. **Yuan Y, Zhao H.** 25 April 2013. Directed evolution of a highly efficient cellobiose utilizing pathway in an industrial *Saccharomyces cerevisiae* strain. Biotechnol. Bioeng. **doi:**10.1002/bit.24946.
15. **Du J, Yuan Y, Si T, Lian J, Zhao H.** 2012. Customized optimization of metabolic pathways by combinatorial transcriptional engineering. Nucleic Acids Res. **40:**e142.
16. **Eriksen DT, Hsieh PCH, Lynn P, Zhao H.** 2013. Directed evolution of a cellobiose utilization pathway in *Saccharomyces cervisiae* by simultaneously engineering multiple proteins. Microb. Cell Fact. **12:**61.
17. **Eriksen DT, Lian J, Zhao H.** 1 April 2013. Protein design for pathway engineering. J. Struct. Biol. **doi:**10.1016/j.jsb.2013.1003.1011.
18. **Wen F, Nair NU, Zhao H.** 2009. Protein engineering in designing tailored enzymes and microorganisms for biofuels production. Curr. Opin. Biotechnol. **20:**412-419.
19. **Cobb RE, Si T, Zhao H.** 2012. Directed evolution: an evolving and enabling synthetic biology tool. Curr. Opin. Chem. Biol. **16:**285-291.
20. **Cobb RE, Sun N, Zhao H.** 2013. Directed evolution as a powerful synthetic biology tool. Methods **60:**81-90.
21. **Cobb RE, Chao R, Zhao H.** 2013. Directed evolution: past, present and future. AIChE J. **59:**1432-1440.
22. **Hillebrecht JR, Wise KJ, Koscielecki JF, Birge RR.** 2004. Directed evolution of bacteriorhodopsin for device applications. Methods Enzymol. **388:**333-347.
23. **Wise KJ, Gillespie NB, Stuart JA, Krebs MP, Birge RR.** 2002. Optimization of bacteriorhodopsin for bioelectronic devices. Trends Biotechnol. **20:**387-394.
24. **Bokma E, Koronakis E, Lobedanz S, Hughes C, Koronakis V.** 2006. Directed evolution of a bacterial efflux pump: adaptation of the *E. coli* TolC exit duct to the *Pseudomonas* MexAB translocase. FEBS Lett. **580:**5339-5343.
25. **Foo JL, Leong SS.** 2013. Directed evolution of an *E. coli* inner membrane transporter for improved efflux of biofuel molecules. Biotechnol. Biofuels **6:**81.
26. **Ren C, Chen T, Zhang J, Liang L, Lin Z.** 2009. An evolved xylose transporter from *Zymomonas mobilis* enhances sugar transport in *Escherichia coli*. Microb. Cell Fact. **8:**66.
27. **Young EM, Comer AD, Huang H, Alper HS.** 2012. A molecular transporter engineering approach to improving xylose catabolism in *Saccharomyces cerevisiae*. Metab. Eng. **14:**401-411.
28. **Lian J, Ma Y, Cai J, Wu M, Wang J, Wang X, Xu Z.** 2009. High-level expression of soluble subunit b of F_1F_0 ATP synthase in *Escherichia coli* cell-free system. Appl. Microbiol. Biotechnol. **85:**303-311.
29. **Xu Z, Lian J, Cai J.** 2010. Efficient expression of aquaporin Z in *Escherichia coli* cell-free system using different fusion vectors. Protein Pept. Lett. **17:**181-185.
30. **Lian J, Ding S, Cai J, Zhang D, Xu Z, Wang X.** 2009. Improving aquaporin Z expression in Escherichia coli by fusion partners and subsequent condition optimization. Appl. Microbiol. Biotechnol. **82:**463-470.
31. **Kai L, Kaldenhoff R, Lian J, Zhu X, Dotsch V, Bernhard F, Cen P, Xu Z.** 2010. Preparative scale production of functional mouse aquaporin 4 using different cell-free expression modes. PLoS One **5:**e12972.

32. **Zhang F, Rodriguez S, Keasling JD.** 2011. Metabolic engineering of microbial pathways for advanced biofuels production. Curr. Opin. Biotechnol. **22:**775-783.
33. **Handke P, Lynch SA, Gill RT.** 2011. Application and engineering of fatty acid biosynthesis in *Escherichia coli* for advanced fuels and chemicals. Metab. Eng. **13:**28-37.
34. **Tehlivets O, Scheuringer K, Kohlwein SD.** 2007. Fatty acid synthesis and elongation in yeast. Biochim. Biophys. Acta **1771:**255-270.
35. **Schirmer A, Rude MA, Li X, Popova E, del Cardayre SB.** 2010. Microbial biosynthesis of alkanes. Science **329:**559-562.
36. **Steen EJ, Kang Y, Bokinsky G, Hu Z, Schirmer A, McClure A, Del Cardayre SB, Keasling JD.** 2010. Microbial production of fatty-acid-derived fuels and chemicals from plant biomass. Nature **463:**559-562.
37. **Runguphan W, Keasling JD.** 27 July 2013. Metabolic engineering of *Saccharomyces cerevisiae* for production of fatty acid-derived biofuels and chemicals. Metab. Eng. **doi:**10.1016/j.ymben.2013.1007.1003.
38. **Lennen RM, Pfleger BF.** 2012. Engineering *Escherichia coli* to synthesize free fatty acids. Trends Biotechnol. **30:**659-667.
39. **Lee SH, Stephens JL, Paul KS, Englund PT.** 2006. Fatty acid synthesis by elongases in trypanosomes. Cell **126:**691-699.
40. **Lee SH, Stephens JL, Englund PT.** 2007. A fatty-acid synthesis mechanism specialized for parasitism. Nat. Rev. Microbiol. **5:**287-297.
41. **Inui H, Miyatake K, Nakano Y, Kitaoka S.** 1984. Fatty acid synthesis in mitochondria of *Euglena gracilis*. Eur. J. Biochem. **142:**121-126.
42. **Hoffmeister M, Piotrowski M, Nowitzki U, Martin W.** 2005. Mitochondrial trans-2-enoyl-CoA reductase of wax ester fermentation from *Euglena gracilis* defines a new family of enzymes involved in lipid synthesis. J. Biol. Chem. **280:**4329-4338.
43. **Chan DI, Vogel HJ.** 2010. Current understanding of fatty acid biosynthesis and the acyl carrier protein. Biochem. J. **430:**1-19.
44. **Gago G, Diacovich L, Arabolaza A, Tsai SC, Gramajo H.** 2011. Fatty acid biosynthesis in actinomycetes. FEMS Microbiol. Rev. **35:**475-497.
45. **Lu JZ, Lee PJ, Waters NC, Prigge ST.** 2005. Fatty acid synthesis as a target for antimalarial drug discovery. Comb. Chem. High T. Scr. **8:**15-26.
46. **Dellomonaco C, Clomburg JM, Miller EN, Gonzalez R.** 2011. Engineered reversal of the beta-oxidation cycle for the synthesis of fuels and chemicals. Nature **476:**355-359.
47. **Clomburg JM, Vick JE, Blankschien MD, Rodriguez-Moya M, Gonzalez R.** 2012. A synthetic biology approach to engineer a functional reversal of the beta-oxidation cycle. ACS Synth. Biol. **1:**541-554.

Chapter 2 Directed Evolution of a Cellodextrin Transporter for Improved Biofuel Production under Anaerobic Conditions in *Saccharomyces cerevisiae*

2.1 Introduction

Introduction of a cellobiose utilization pathway consisting of a cellodextrin transporter and a β-glucosidase into *Saccharomyces cerevisiae* enables co-fermentation of cellobiose and xylose (1, 2). Cellodextrin transporter 1 (CDT1) from *Neurospora crassa* has been established as an effective transporter for the engineered cellobiose utilization pathways (1-8). However, cellodextrin transporter 2 (CDT2) from the same species is a facilitator and has the potential to be more efficient than CDT1 under anaerobic conditions due to its energetic benefits (9). Currently, CDT2 has a very low activity and is considered rate-limiting in cellobiose fermentation. In this chapter, directed evolution of CDT2 was carried out to increase cellobiose uptake activity and anaerobic cellobiose fermentation performance.

First of all, a high throughput screening method based on colony size was developed to engineer the cellodextrin transporter. Owing to the important role of the sugar utilization pathway on cellular metabolism, the activity of the fermenting pathway can be coupled to the growth rate on a specific sugar, such as cellobiose and xylose. Therefore, the enrichment or adaptive evolution methods were commonly used to engineer efficient sugar fermenting strains (10). Despite the success in constructing efficient cellobiose (4, 5) or xylose (11-13) fermenting yeasts, the improved phenotypes are often found to be related to the modification of the host genome rather than the engineered pathway, and it is rather difficult to figure out the molecular mechanisms of the random modifications. To minimize the impact of host adaptation, a colony size based screening method was developed in our group to engineer efficient sugar utilization

pathways (6, 8). Sugar uptake is the first step of cellular metabolism, and it is generally assumed that transporter is rate-limiting in the whole fermentation pathway (4, 7, 14, 15). Therefore, the colony size based screening method was also applied to engineer the cellobiose transporter.

Using the developed high throughput screening method, three rounds of directed evolution of CDT2 was carried out, and the cellobiose uptake activity of CDT2 was increased by 2.15 fold, which resulted from both increased specific activity and transporter expression level. Under anaerobic conditions with high cell density, the evolved mutant conferred significantly improved cellobiose fermentation performance, with the sugar consumption rate and ethanol productivity increased by 2.67 fold and 4.96 fold, respectively.

2.2 Results

2.2.1 Construction of Cellobiose Utilization Pathways

The yeast homologous recombination based DNA assembler method (16) was used to construct recombinant plasmids and a library of CDT2 mutants. Oligonucleotides used and strains and plasmids constructed are listed in Appendix and Table 2.1, respectively.

Table 2.1 Strains and plasmids constructed in this study.

Name	Description
Strains	
INV*Sc*1	*MATa/MATα his3Δ1/his3Δ1 leu2/leu2 trp1-289/trp1-289 ura3-52/ura3-52*
DH5α	F– Φ80*lacZ*ΔM15 Δ(*lac*ZYA-*arg*F) U169 *rec*A1 *end*A1 *hsd*R17 (rK–, mK+) *pho*A *sup*E44 λ– *thi*-1 *gyr*A96 *rel*A1
Plasmids	
pRS415	Single copy plasmid in *S. cerevisiae* with *LEU2* marker
pRS425-801	Plasmid with the *TEF1p-NCU00801-PGK1t* cassette
pRS425-809	Plasmid with the *TEF1p-NCU00809-PGK1t* cassette
pRS425-8114	Plasmid with the *TEF1p-NCU08114-PGK1t* cassette
CDT-Eng-H	pRS415-*PYK1p-NCU00130-ADH1t-TEF1p-Pst*I-*PGK1t*
CDT1-BGL	*NCU00801(CDT1)* inserted into CDT-Eng-H
NCU00809-BGL	*NCU00809* inserted into CDT-Eng-H
CDT2-BGL (WT)	*NCU08114 (CDT2)* inserted into CDT-Eng-H
QFN	*CDT2*(Q207H/F209I/N311H) inserted into CDT-Eng-H
Q	*CDT2*(Q207H) inserted into CDT-Eng-H
F	*CDT2*(F209I) inserted into CDT-Eng-H
N	*CDT2*(N311H) inserted into CDT-Eng-H
QF	*CDT2*(Q207H/F209I) inserted into CDT-Eng-H
QN	*CDT2*(Q207H/N311H) inserted into CDT-Eng-H
FN	*CDT2*(F209I/N311H) inserted into CDT-Eng-H
QNI	*CDT2*(Q207H/N311H/I505T) inserted into CDT-Eng-H
WT-eGFP	*CDT2-eGFP* inserted into CDT-Eng-H
QFN-eGFP	*CDT2*(Q207H/F209I/N311H)-*eGFP* inserted into CDT-Eng-H
QN-eGFP	*CDT2*(Q207H/N311H)-*eGFP* inserted into CDT-Eng-H
QNI-eGFP	*CDT2*(Q207H/N311H/I505T)-*eGFP* inserted into CDT-Eng-H

To facilitate the construction of cellobiose utilization pathways, a helper plasmid with the functional elements *PYK1p-NCU00130-ADH1t-TEF1p-Pst*I-*PGK1t* cloned into pRS415 was constructed, named CDT-Eng-H hereafter (Figure 2.1). *NCU00130* is a *N. crassa* gene encoding β-glucosidase and expressed intra-cellularly in *S. cerevisiae*. The helper plasmid was linearized by *Pst*I digestion to allow the insertion of cellodextrin transporters. *NCU00801*, *NCU00809*, and *NCU08114* were cloned from pRS425-801, pRS425-809, and pRS425-8114 constructed in our previous studies (2), respectively, using primers oJL0099 and oJL0100.

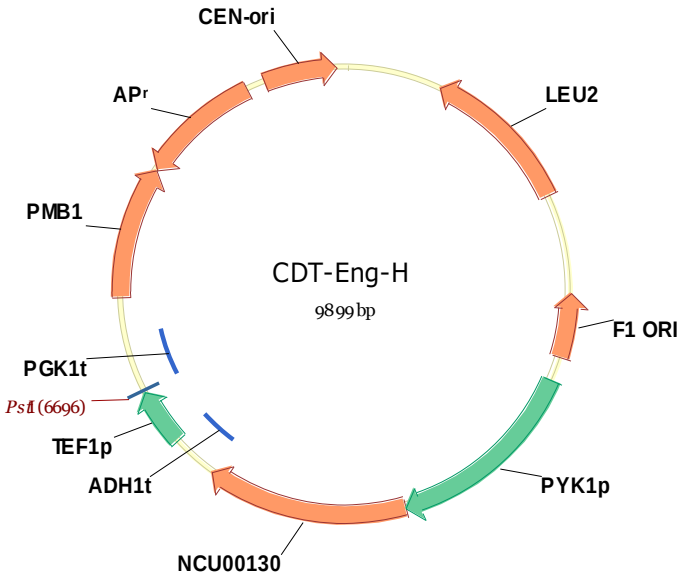

Figure 2.1 Vector map of the helper plasmid for CDT2 engineering, CDT-Eng-H. NCU00130 is the β-glucosidase from *N. crassa*, and the cellobiose utilization pathways are constructed by inserting cellodextrin transporters into the *Pst*I site, which was flanked by *TEF1* promoter and *PGK1* terminator.

2.2.2 Development of a Colony Size Based Screening Method for CDT Engineering

A colony size based screening method was developed previously to engineer efficient sugar utilization pathways (6, 8), which was also applied to engineer the cellodextrin transporter. Before performing directed evolution, this method was characterized using three *N. crassa* cellodextrin transporters with different activities, including NCU00801 (CDT1), NCU00809, and NCU08114 (CDT2) (9). In accordance with the previous work (1, 2), CDT1 performed the best in cellobiose fermentation, followed by CDT2 and then NCU00809, under aerobic conditions. After spreading onto a cellobiose plate, the colony size was correlated with the growth rate in liquid medium, and therefore the cellobiose uptake activity (Figure 2.2). These results also confirmed that CDT2 was rate-limiting in cellobiose fermentation under the screening conditions.

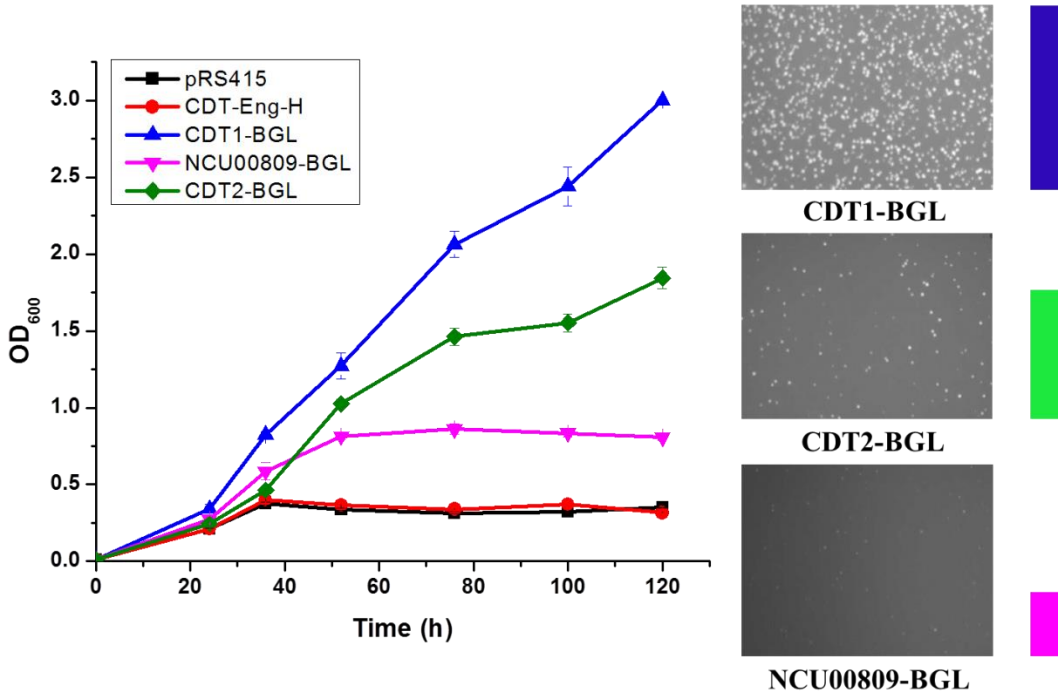

Figure 2.2 Development of a colony size based screening method for CDT engineering. Different CDTs were introduced into CDT-Eng-H, a plasmid containing the β-glucosidase (BGL) from *N. crassa*. The colony size on cellobiose agar plate (middle panel) was confirmed to be positively related to the growth rate in liquid culture (left panel), as well as the cellobiose uptake activity (right panel). Bars on the right panel represented the relative cellobiose uptake activity (9), with CDT1 activity set to 100%.

2.2.3 CDT2 Engineering via Directed Evolution

Using the colony size based screening method, a general protocol for CDT2 engineering was developed (Figure 2.3). Error-prone PCR (17) was used to create a library of CDT2 mutants, which was then cloned into linearized CDT-Eng-H. The concentration of $MnCl_2$ was adjusted to keep the mutation rate around 3 bp per kb (4-5 bp per gene). After heat shock, a small amount of the transformant culture (0.1%) was spread onto an SCD-Leu plate to determine the library size. Under optimal conditions, 500 ng for each DNA fragment, a library ranging from 10^5 to 10^6 transformants could be obtained. The rest of the transformants were diluted appropriately, and around 10^4 transformants were spread onto SCC-Leu agar plates. After incubation at 30 ℃ for 3 days, many large colonies appeared and the top 60 colonies were picked and pre-cultured in

SCD-Leu medium. After growth to saturation, cells were inoculated into 3 mL YPC liquid medium in culture tubes and samples were taken at 24h, 28h, and 32h after inoculation to determine the cell density and specific growth rate. The top 12 mutants with either the highest cell density or specific growth rate were selected and the plasmids were extracted and re-transformed into fresh yeast cells to eliminate host adaptation. After re-transformation, the selected mutants were further confirmed using flask fermentation under oxygen limited conditions (10 mL YPC medium in 50 mL un-baffled flask) and samples were taken at 24h, 28h, 32h, and 36h after inoculation to measure cell density, cellobiose consumption, and ethanol productivity. The top 3 mutants with the highest cellobiose consumption and ethanol production rates were selected for final characterization under anaerobic conditions. The anaerobic tube was filled with 10 mL YPC medium and samples were taken every day until all sugar was consumed. In the whole process of library screening, seed cultures were grown in 3 mL SCD-Leu medium under aerobic conditions for 36 hours in 14 mL culture tubes, and inoculated into YPC at an initial OD_{600} of 0.05. Iterative rounds of directed evolution were carried out until no further improvement was observed.

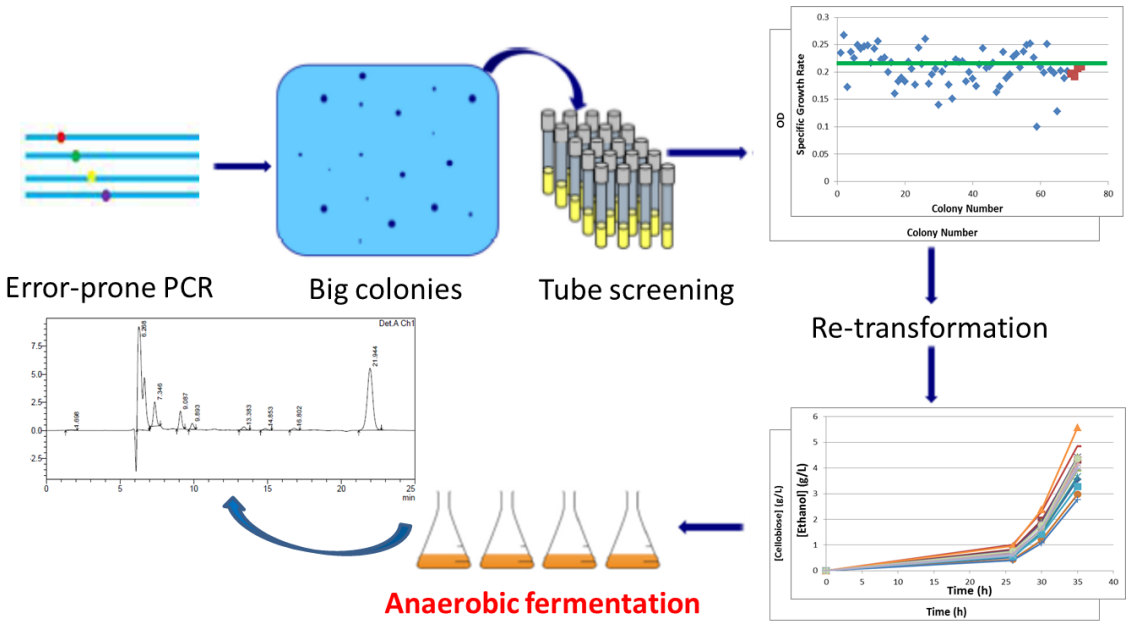

Figure 2.3 A general scheme to engineer sugar transporters, using the colony size based screening method.

For easier operation and based on the assumption that oxygen level cannot significantly change the activity of a facilitator, the initial screening steps were carried out under aerobic or oxygen-limited conditions, and only the final step of confirmation was performed under anaerobic conditions. In the first round of directed evolution, the top 2 mutants were found to carry the same mutations, Q207H/F209I/N311H (QFN), which validated the developed protocol for cellobiose transporter engineering. The role of these mutations in cellobiose fermentation was analyzed by creating all different combinations of the mutations including Q207H (Q), F209I (F), N311H (N), Q207H/F209I (QF), Q207H/N311H (QN), and F209I/N311H (FN). As shown in Figure 2.4, variants QN, QFN, N, and Q grew faster than the wild-type CDT2 (WT), while variants QF and F grew slower than WT. Accordingly, it can be concluded that Q207H and N311H are beneficial mutations, whereas the F209I mutation impairs the cellobiose uptake activity.

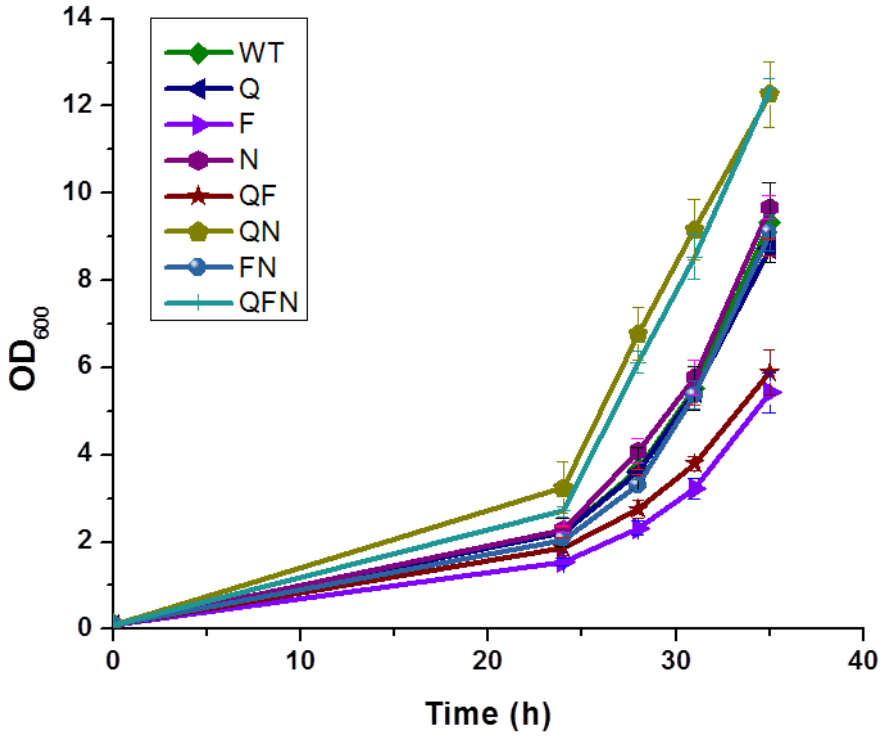

Figure 2.4 Characterization of the role of Q207H/F209I/N311H (QFN) mutations in cellobiose fermentation performance by creating all possible combinations, including Q207H (Q), F209I (F), N311H (N), Q207H/F209I (QF), Q207H/N311H (QN), and F209I/N311H (FN).

Using the mutants obtained in the second round of directed evolution, the cellobiose fermentation performance was compared under aerobic, oxygen-limited, and anaerobic conditions. In agreement with our assumption that the activity of a facilitator is not significantly changed by the oxygen level, the growth and cellobiose consumption rates of these mutants were closely correlated under different conditions (Figure 2.5).

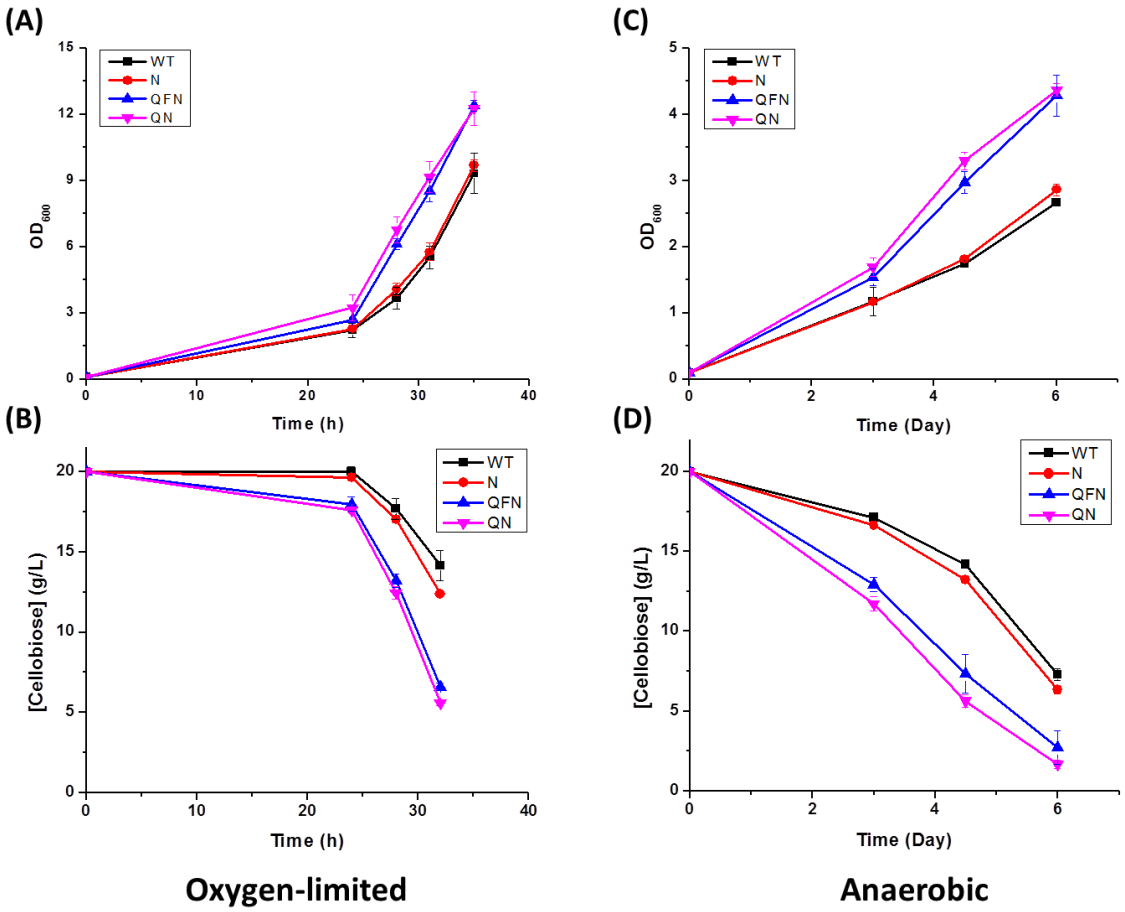

Figure 2.5 Correlation of cellobiose fermentation performance under oxygen-limited and anaerobic conditions. Growth curve (A, C) and cellobiose consumption profile (B, D) were determined under both oxygen-limited (A, B) and anaerobic conditions (C, D).

After validating our developed protocol for CDT engineering, a third round of directed evolution was carried out using the best mutant, QN, as the template. Similarly, mutants with increased cellobiose consumption rate were obtained, and DNA sequencing revealed that the best mutant harbored only one additional mutation, I505T, named QNI hereafter. The fourth round of directed evolution did not result in mutants with significantly improved cellobiose fermentation performance (data not shown), thus further rounds of directed evolution of CDT2 was not continued.

2.2.4 Cellobiose Fermentation Performance of the Evolved CDT2 Mutants

The cellobiose fermentation performance (sugar consumption rate, ethanol productivity and yield) of WT and the best mutants obtained in the first (QFN), second (QN), and third (QNI) round of directed evolution was compared under anaerobic conditions. Using the same conditions as library screening, the specific growth rate, sugar consumption rate, and ethanol productivity were increased by 2.15 fold, 2.65 fold, and 4.69 fold, respectively (Figure 2.6).

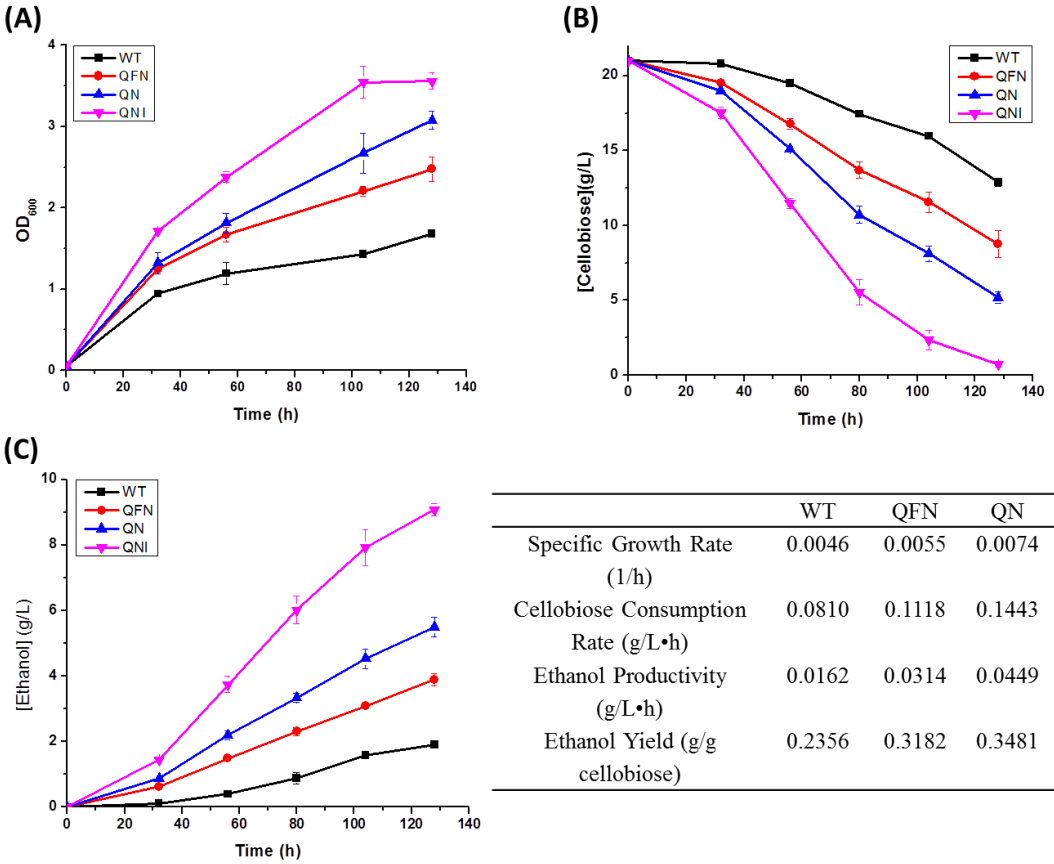

	WT	QFN	QN	QNI
Specific Growth Rate (1/h)	0.0046	0.0055	0.0074	0.0099
Cellobiose Consumption Rate (g/L•h)	0.0810	0.1118	0.1443	0.2145
Ethanol Productivity (g/L•h)	0.0162	0.0314	0.0449	0.0760
Ethanol Yield (g/g cellobiose)	0.2356	0.3182	0.3481	0.4476

Figure 2.6 Cellobiose fermentation profiles of CDT2 mutants obtained in the first (QFN), second (QN), and third (QNI) round of directed evolution. The specific growth rate (A), cellobiose consumption rate (B), and ethanol productivity (C) of these transporters were compared using the library screening conditions. Ethanol used to solubilize anaerobic growth factors (0.5-1 g/L) was subtracted before calculating ethanol productivity and ethanol yield. To determine the specific growth rate, cellobiose consumption rate and ethanol productivity, data points within linear range were included for analysis. Final data points were used to determine ethanol yield.

If a high cell density was used for anaerobic fermentation, the strain containing the evolved transporter was able to consume 20 g/L cellobiose in less than 9 hours, while the wild-type transporter required more than 30 hours to use up the same amount of cellobiose. The best mutant (QNI) conferred an increase of 2.67 fold and 4.96 fold for the cellobiose consumption rate and ethanol productivity, respectively (Figure 2.7). Moreover, the overall ethanol yield, which is another important parameter for cost-effective production of cellulosic biofuels, was improved by more than 25%.

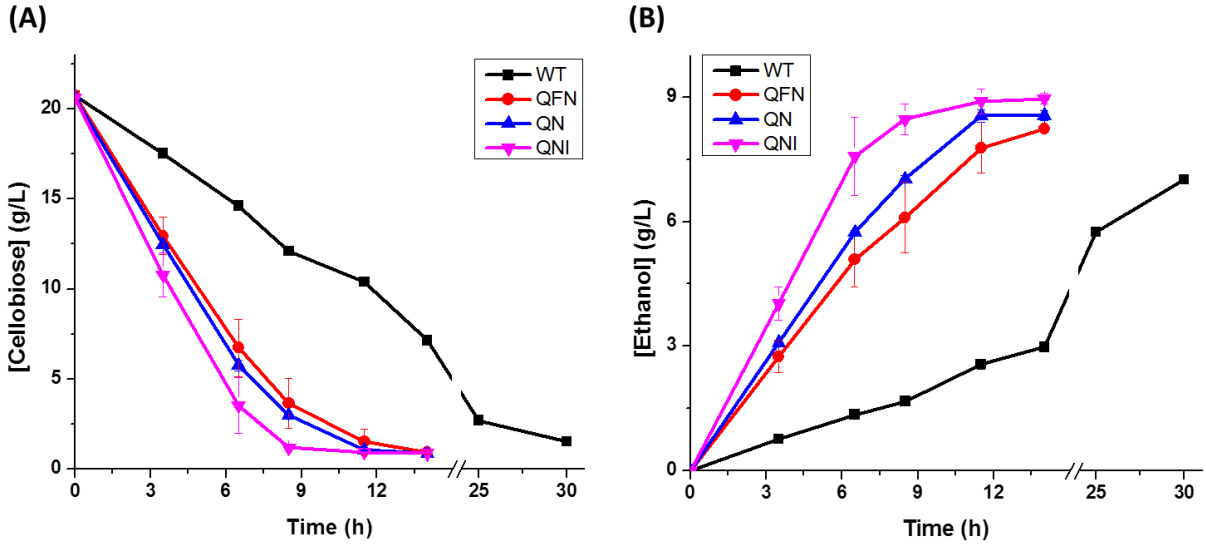

	WT	QFN	QN	QNI
Cellobiose Consumption Rate (g/L·h)	0.9567±0.0062	1.98435±0.076	2.1141±0.0080	2.5506±0.3337
Ethanol Productivity (g/L·h)	0.2350±0.0017	0.6079±0.0205	0.7562±0.0062	1.1655±0.1436
Ethanol Yield (g/g cellobiose)	0.3643±0.0071	0.4150±0.0043	0.4328±0.0018	0.4536±0.0109

Figure 2.7 Cellobiose fermentation profiles of CDT2 mutants obtained in the first (QFN), second (QN), and third (QNI) round of directed evolution. The cellobiose consumption rate (A) and ethanol productivity (B) of these transporters were compared using high cell density fermentation under anaerobic conditions. Ethanol produced by CDT2 mutants represented the total ethanol in the fermentation broth subtracted by ethanol used to solubilize the anaerobic growth factors (0.5-1 g/L).

2.2.5 Characterization of the Evolved CDT2 Mutants

To investigate the role of mutations on cellobiose fermentation and cellobiose uptake activity, we first determined the relative expression levels of CDT2 and its mutants. To fuse enhanced green fluorescent protein (eGFP) at the C-terminus of the cellodextrin transporters with a Gly-Ser-Gly-Ser linker in between, primers oJL0099 and oJL0154 were used to amplify the *CDT2* fragment and oJL0155 and oJL0100 to amplify the *eGFP* fragment, respectively, which were then cloned into the linearized CDT-Eng-H using the DNA assembler method. As shown in Figure 2.8A, the cytoplasmic membrane localization of the transporter-eGFP fusion proteins was confirmed by confocal microscope imaging. Therefore, the relative expression levels of the cellodextrin transporters could be quantified by their fluorescence intensity. Under cellobiose fermentation conditions, the expression levels of WT, QFN, and QN were similar, while the expression level of QNI was about 18% higher (Figure 2.8B).

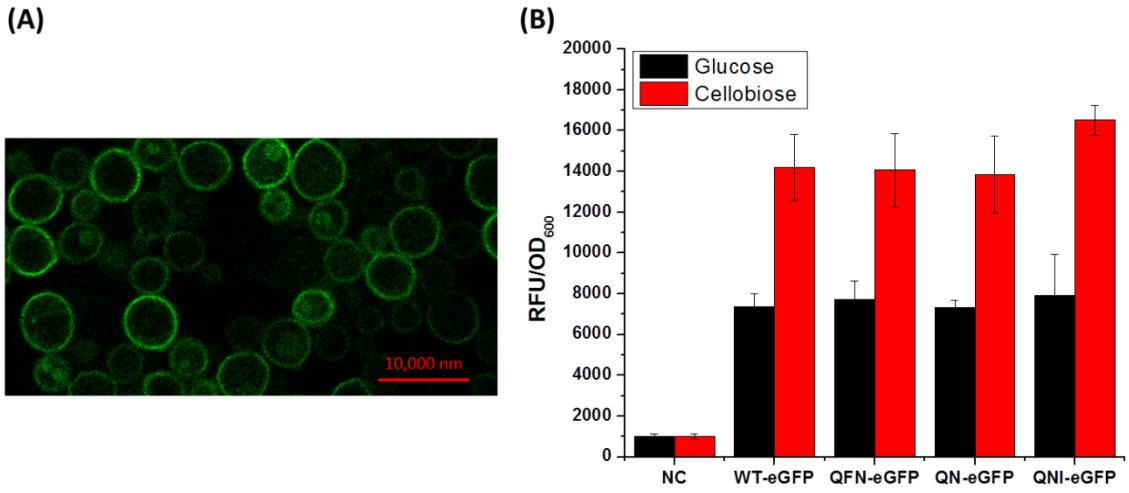

Figure 2.8 Cytoplasmic membrane localization of the CDT2-eGFP fusion protein and relative expression levels of cellodextrin transporters quantified by eGFP relative fluorescence unit (RFU). A) Confocal microscope image of yeast cells expression WT-eGFP cultured in cellobiose medium. B) Relative expression levels of cellodextrin transporters in both glucose medium and cellobiose medium. NC is the control strain (WT) without eGFP tagging.

To further correlate the sugar uptake activity and the cellobiose fermentation performance, the cellobiose uptake activity of WT, QFN, QN, and QNI was determined by the oil stop method. As expected, the cellobiose uptake activity was correlated with the fermentation performance, i.e. higher activity resulted in increased specific growth rate, cellobiose consumption rate, and ethanol productivity (Figure 2.9A). By normalizing the transporter activity to the relative protein expression level, it was found that the specific activity of QN and QNI were nearly the same, indicating that Q207H and N311H increased the specific uptake activity, while I505T contributed to increased transporter expression level (Figure 2.9B). Notably, the absolute value of cellobiose uptake activity (WT) was higher than that reported (9), which could be caused by the difference in culture conditions. In the previous work, the strain was pre-cultured in glucose medium, while cellobiose medium was used in the present study. As a selection pressure, cellobiose could lead to higher transporter expression level, as shown in Figure 2.8B. It was also found that cellodextrin transporters suffered from degradation when glucose was used as the carbon source (personal communication with Prof. Yong-Su Jin). Therefore, the enhanced expression level and increased protein stability might explain the higher cellobiose uptake activity observed in the current study.

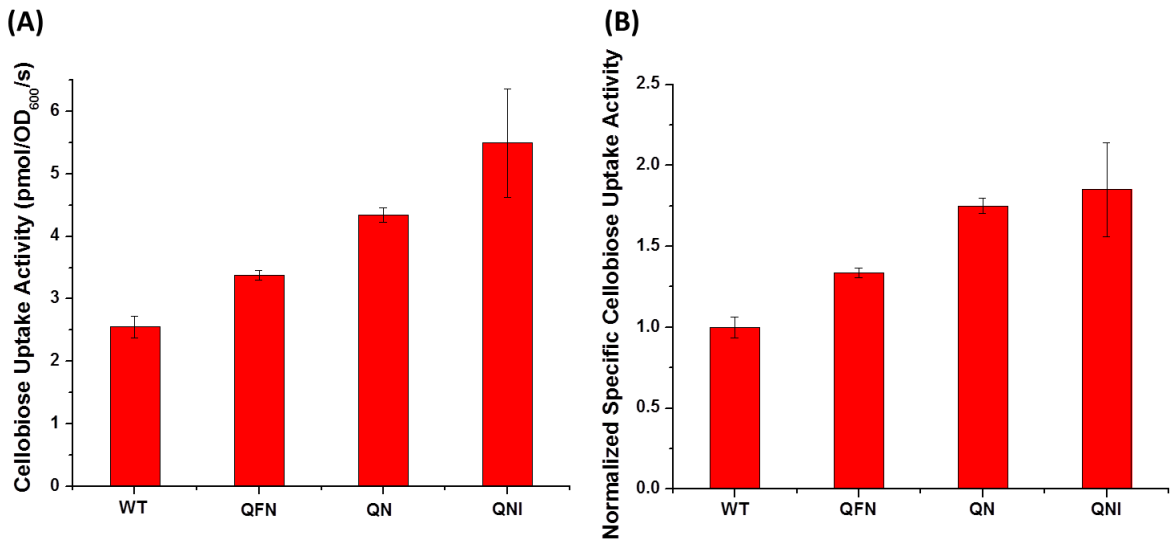

Figure 2.9 Cellobiose uptake activity of CDT2 mutants. Sugar uptake assay was performed using [^{3}H]-Cellobiose and normalized to either cellular level (A) or protein level (B). For the transporter activity at cellular level, cellobiose uptake assay was performed at OD_{600} 1. Cellobiose uptake activity at the protein level (B) was normalized to the relative transporter expression level, which was quantified by fluorescence intensity (the specific cellobiose uptake activity of WT-eGFP was set to 1).

2.3 Discussion

Intensive research has been focused on producing fuels and chemicals from lignocellulose biomass (18, 19). To make the cellulosic biofuel fermentation process economically feasible, the host should be able to consume a mixture of sugars efficiently and simultaneously. However, the presence of glucose repression significantly impairs the efficiency and productivity, which is considered as one of the major obstacles for cost-effective production of cellulosic biofuels. Three general strategies are proposed to overcome glucose repression to allow co-fermentation of mixed sugars (20): the construction of glucose-derepressed yeasts by perturbing the glucose sensing and signaling network, the introduction and engineering of xylose specific transporters, and the introduction of a cellobiose utilization pathway including a cellodextrin transporter and a β-glucosidase. Due to the complexity of the regulatory system, yeast strains without glucose repression on xylose metabolism have never been obtained, even after intensive systematic

metabolic engineering (20, 21). As for xylose transporters, they suffer from either low uptake activity or low specificity (14, 22), and it is assumed that xylose specific transporters with high uptake activity may not exist in nature (15, 20). Although directed evolution was carried out on xylose transporters, efficient co-fermentation of glucose and xylose has not been achieved either (15). On the contrary, the last strategy has been proven to be an efficient strategy to overcome glucose repression, enabling co-fermentation of cellobiose/xylose (1, 2) and cellobiose/galactose (3) efficiently. Another advantage of the cellobiose pathway is the application in consolidated bioprocessing (simultaneous saccharification and fermentation, SSF), because the utilization of cellobiose instead of glucose can eliminate the requirement of β-glucosidase supplementation in current cellulase cocktails (9).

Although there are numerous protein engineering examples (23-25), there are only a few examples of engineering membrane proteins, especially transporters (15, 26-28). As the bridge between intra- and extra-cellular environments, membrane proteins are mainly involved in the transduction of extra-cellular signals, transportation of substances through membrane, and generation of energy, whose activities are difficult or labor-intensive to determine (29, 30). Thus, directed evolution is limited by the difficulty in determining the activity of membrane proteins, let alone the development of a high-throughput screening system. Fortunately, sugar transporters are essential to initiate the cellular metabolism, and a high throughput screening method based on cell growth rate can be readily developed (Figure 2.2 and Figure 2.3). Using this high-throughput screening system, cellobiose fermentation performance (Figure 2.6) and cellobiose uptake activity (Figure 2.7) were significantly improved after three rounds of directed evolution. Due to the lack of 3-D structure of cellodextrin transporters, the HMMTOP online tool (31) and the TMRPres2D tool (32) were used to predict and visualize the secondary structure of CDT2.

Based on the predicted topology, Q207 and N311 were located in the sixth and seventh transmembrane helixes, while I505 was located in the last intra-cellular loop (Figure 2.10). The predicted positions of these mutations were consistent with their corresponding roles: the inner membrane located residues might be involved in the cellobiose channel formation and affect the specific uptake activity, while the residue in the intra-cellular loop might not be related to cellobiose uptake directly. Previous work on transporter engineering also revealed that the mutation in the intra-cellular loops could increase the sugar uptake activity (7, 15), which might result from increased transporter expression levels.

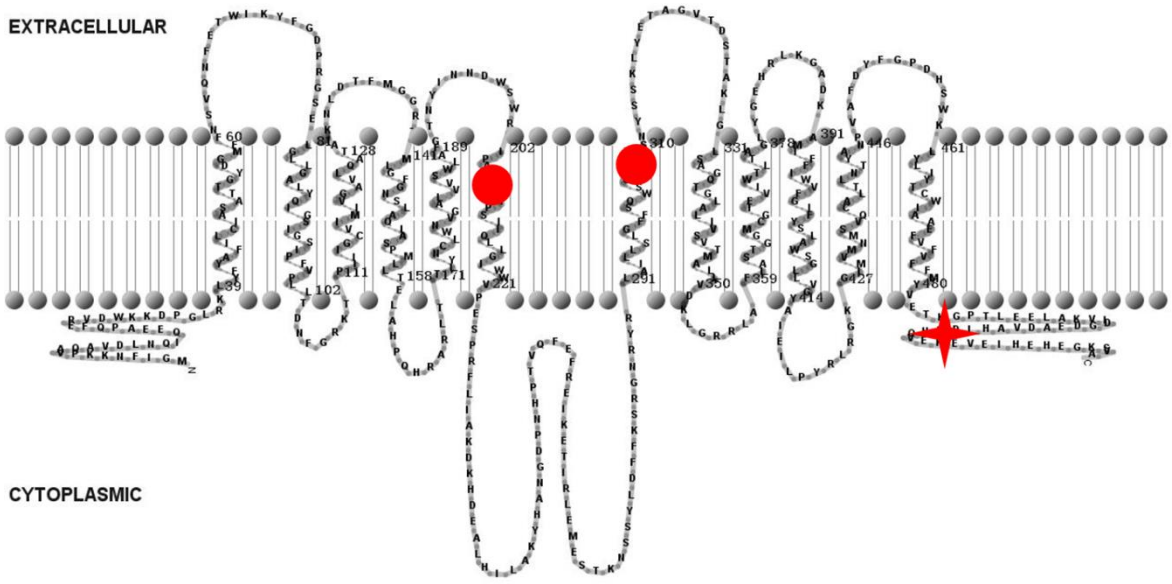

Figure 2.10 Sequence-structure mapping of CDT2 mutations. The topology of CDT2 on cellular membrane was predicted by HMMTOP online program. The ovals indicate the mutations obtained in the first two rounds of directed evolution, while the star represents the third round mutation.

Recently, a bacterial cellobiose phosphorylase together with a highly functional CDT1 mutant were introduced into *S. cerevisiae* and confirmed to perform better than the hydrolytic pathway under low oxygen or acetate supplemented conditions (4). The energy requirement of CDT1 for cellobiose uptake could be to some extent compensated by the phosphorolytic pathway

under stress conditions, owing to the energetic benefits of cellobiose phosphorolysis. In the hydrolytic pathway, cellobiose is cleaved by β-glucosidase to generate two glucose molecules, which need to be phosphorylated by 2 ATP molecules (per cellobiose) to enter glycolysis. In the phosphorolytic pathway, cellobiose is cleaved by phosphorylase to release one glucose molecule and one glucose-1-phophate molecule, and only one ATP molecule (per cellobiose) is consumed to initiate fermentation (33). Despite the energetic benefits, a CDT1 mutant with significantly improved uptake activity was necessary to provide a "push" driving force to enable efficient cellobiose fermentation (4). Therefore, a cellobiose pathway combining the engineered CDT2 with cellobiose phosphorylase may have the maximized energetic benefits, and further improve cellobiose fermentation performance under anaerobic conditions.

2.4 Conclusions

In summary, the cellobiose uptake activity of CDT2 was increased via directed evolution to improve anaerobic cellobiose fermentation performance, including the specific growth rate, cellobiose consumption rate, ethanol productivity, and ethanol yield. For the best mutant (QNI) obtained after three rounds of directed evolution, the two mutations located in transmembrane helixes conferred a 1.75 fold increase in the specific cellobiose uptake activity, while the mutation in the intra-cellular loop was determined to increase the transporter expression level rather than the specific activity. To our knowledge, this is the first report of using directed evolution to increase the activity of a cellodextrin transporter and the productivity of cellulosic biofuels under anaerobic conditions.

2.5 Materials and Methods

2.5.1. Strains, Media, and Cultivation Conditions

E. coli strain DH5α (Life Technologies, Grand Island, NY) was used to maintain and amplify plasmids. *S. cerevisiae* INV*Sc*1 strain (Life Technologies) was used as the host for homologous recombination based cloning and cellobiose fermentation. Yeast strains were cultivated in complex medium consisting of 2% peptone and 1% yeast extract supplemented with either 2% glucose (YPD) or 2% cellobiose (YPC). Recombinant strains were grown on synthetic complete medium consisting of 0.17% yeast nitrogen base, 0.5% ammonium sulfate, and 0.07% amino acid drop out mix without leucine (CSM-Leu, MP Biomedicals, Solon, OH), supplemented with 2% glucose (SCD-Leu) or 2% cellobiose (SCC-Leu). *E. coli* strains were cultured at 37^{o}C in Luria-Bertani broth containing 100 μg/mL ampicillin. *S. cerevisiae* strains were cultured at 30^{o}C and 250 rpm for aerobic growth, and 30^{o}C and 100 rpm in un-baffled shaker flasks for oxygen limited fermentation. For anaerobic fermentation, anaerobic culture tubes with butyl rubber stoppers and aluminum seals (Chemglass Life Sciences, Vineland, NJ) were vacuumed and purged with nitrogen to remove the residual oxygen and 480 mg/L Tween-80 and 10 mg/L ergosterol were supplemented as anaerobic growth factors (34). Tween-80 and ergosterol were dissolved in ethanol, and the supplementation resulted in around 0.5-1 g/L ethanol in the fermentation broth. Go Taq DNA polymerase for error-prone PCR was purchased from Promega (Madison, WI). All restriction enzymes, Q5 High Fidelity DNA polymerase, and the *E. coli* - *S. cerevisiae* shuttle vector, pRS415, were purchased from New England Biolabs (Ipswich, MA). All chemicals were purchased from either Sigma-Aldrich or Fisher Scientific.

2.5.2 DNA Manipulation

The yeast homologous recombination based DNA assembler method (16) was used to construct recombinant plasmids and a library of CDT2 mutants. Briefly, Polymerase chain reaction (PCR) was used to generate DNA fragments with homology arms at both ends, which were purified with a QIAquick Gel Extraction Kit (Qiagen, Valencia, CA) and co-transformed along with the linearized backbone into *S. cerevisiae*. To confirm the correct clones, yeast plasmids were isolated using a Zymoprep Yeast Plasmid Miniprep II Kit (Zymo Research, Irvine, CA) and re-transformed into *E. coli* DH5α competent cells. Plasmids were isolated using a QIAprep Spin Miniprep Kit (Qiagen) and confirmed using both diagnostic PCR and DNA sequencing. Yeast strains were transformed using the LiAc/SS carrier DNA/PEG (35) method, and transformants were selected on SCD-Leu plates.

2.5.3 High Cell Density Fermentation

A single colony from the newly transformed plate was inoculated into 3 mL SCD-Leu medium, and cultured under aerobic conditions for 36 h. Then 1 mL seed culture was used to inoculate 15 mL YPC medium in a shake flask and cultured for an additional 24 h. The late-log phase cells were harvested and washed twice in double distilled water (ddH_2O), and inoculated into 10 mL YPC medium at an initial OD_{600} of 10 in a 20 mL anaerobic culture tube. Cellobiose fermentation was performed under anaerobic conditions and samples were taken every 3-4h after inoculation until all cellobiose was consumed.

2.5.4 [^{3}H]-Cellobiose Uptake Assay

Cellobiose transport assay was performed using the oil-stop method as described previously (9). A single colony of a yeast strain expressing a cellodextrin transporter fused to eGFP was pre-grown in SCD-Leu medium for around 36 h, which was then inoculated into 10 mL fresh YPC medium. Mid-log phase cells cultured under oxygen-limited conditions were harvested and washed 3 times with the assay buffer (30 mM MES-NaOH and 50 mM ethanol, pH5.5), and resuspended to an OD_{600} of 20. The uptake assay was initiated by adding 50 μL cells into 50 μL [^{3}H]-cellobiose (Moravek Biochemicals, Brea, CA) layered over 100 μL silicone oil. To stop the reaction, cells were centrifuged for 1 min at 15000 rpm to achieve phase separation, with the cells at the bottom, silicon oil in the middle, and celllobiose solution at the top. Then the tubes were frozen in ethanol/dry ice and the bottom fraction with cell pellets was collected and solubilized in 1 mL NaOH (0.5 M) overnight. Half of the supernatant was transferred into a scintillation vial and 3 mL ScintiSafe* Econo 1 Cocktail (Fisher Scientific) was added to read counts per minute (CPM) by a Beckman LS6500 scintillation counter (Beckman Coulter, Brea, CA). The maximum uptake rate (V_{max}) was determined by measuring the linear rate of cellobiose uptake at the concentration of 400 μM, which is about 100 fold higher than the K_m of CDT2. The value of V_{max} was normalized to both cellular level (cell density) and protein level (protein expression level as quantified by the eGFP fluorescence intensity).

2.5.5 Confocal Microscope Imaging

Yeast cells expressing eGFP tagged cellodextrin transporters were cultured in either glucose or cellobiose medium. A small droplet of mid-log phase cells were transferred onto a pierce of

cover glass and the fluorescence images were taken using a Zeiss LSM 700 Confocal Microscope (Carl Zeiss Microscopy, Thornwood, NY).

2.5.6 Analytical Methods

Cell growth was determined by measuring the absorbance at 600 nm using a Biotek Synergy 2 Multi-Mode Microplate Reader (Winooski, VT), and eGFP fluorescence intensity was measured using a Tecan Safire^2 microplate reader (San Jose, CA) at 488 ± 5 nm and 509 ± 5 nm wavelengths for excitation and emission, respectively. Extra-cellular metabolites, including cellobiose, glucose, acetate, glycerol, and ethanol, were detected and quantified using Shimadzu HPLC (Columbia, MD) equipped with an Aminex HPX-87H column (Bio-Rad, Hercules, CA) and Shimadzu RID-10A refractive index detector. The column was kept at 65^{o}C and 0.5 mM sulfuric acid solution was used as a mobile phase at a constant flow rate of 0.6 mL/min. Each data point represents the mean of at least duplicates.

2.5.7 Prediction of Transporter Topology on Cellular Membrane

The topology of CDT2 on the cellular membrane was predicted using the HMMTOP online tool (http://www.enzim.hu/hmmtop/) (31), and the predicted result was visualized by the TMRPres2D tool (http://bioinformatics.biol.uoa.gr/TMRPres2D/) (32).

2.6 References

1. **Ha SJ, Galazka JM, Kim SR, Choi JH, Yang X, Seo JH, Glass NL, Cate JH, Jin YS.** 2011. Engineered *Saccharomyces cerevisiae* capable of simultaneous cellobiose and xylose fermentation. Proc. Natl. Acad. Sci. U. S. A. **108:**504-509.
2. **Li S, Du J, Sun J, Galazka JM, Glass NL, Cate JH, Yang X, Zhao H.** 2010. Overcoming glucose repression in mixed sugar fermentation by co-expressing a cellobiose transporter and a beta-glucosidase in *Saccharomyces cerevisiae*. Mol. Biosyst. **6:**2129-2132.
3. **Ha SJ, Wei Q, Kim SR, Galazka JM, Cate JH, Jin YS.** 2011. Cofermentation of cellobiose and galactose by an engineered *Saccharomyces cerevisiae* strain. Appl. Environ. Microbiol. **77:**5822-5825.
4. **Ha SJ, Galazka JM, Oh EJ, Kordic V, Kim H, Jin YS, Cate JH.** 2013. Energetic benefits and rapid cellobiose fermentation by *Saccharomyces cerevisiae* expressing cellobiose phosphorylase and mutant cellodextrin transporters. Metab. Eng. **15:**134-143.
5. **Ha SJ, Kim H, Lin Y, Jang MU, Galazka JM, Kim TJ, Cate JH, Jin YS.** 2013. Single amino acid substitutions in HXT2.4 from *Scheffersomyces stipitis* lead to improved cellobiose fermentation by engineered *Saccharomyces cerevisiae*. Appl. Environ. Microbiol. **79:**1500-1507.
6. **Du J, Yuan Y, Si T, Lian J, Zhao H.** 2012. Customized optimization of metabolic pathways by combinatorial transcriptional engineering. Nucleic Acids Res. **40:**e142.
7. **Eriksen DT, Hsieh PCH, Lynn P, Zhao H.** 2013. Directed evolution of a cellobiose utilization pathway in *Saccharomyces cervisiae* by simultaneously engineering multiple proteins. Microb. Cell Fact. **12:**61.
8. **Yuan Y, Zhao H.** 25 April 2013. Directed evolution of a highly efficient cellobiose utilizing pathway in an industrial *Saccharomyces cerevisiae* strain. Biotechnol. Bioeng. **doi:**10.1002/bit.24946.
9. **Galazka JM, Tian C, Beeson WT, Martinez B, Glass NL, Cate JH.** 2010. Cellodextrin transport in yeast for improved biofuel production. Science **330:**84-86.
10. **Cakar ZP, Turanli-Yildiz B, Alkim C, Yilmaz U.** 2012. Evolutionary engineering of *Saccharomyces cerevisiae* for improved industrially important properties. FEMS Yeast Res. **12:**171-182.
11. **Kim SR, Skerker JM, Kang W, Lesmana A, Wei N, Arkin AP, Jin YS.** 2013. Rational and evolutionary engineering approaches uncover a small set of genetic changes efficient for rapid xylose fermentation in *Saccharomyces cerevisiae*. PLoS One **8:**e57048.
12. **Kim SR, Ha SJ, Kong, II, Jin YS.** 2012. High expression of *XYL2* coding for xylitol dehydrogenase is necessary for efficient xylose fermentation by engineered *Saccharomyces cerevisiae*. Metab. Eng. **14:**336-343.
13. **Kim SR, Park YC, Jin YS, Seo JH.** 21 March 2013. Strain engineering of *Saccharomyces cerevisiae* for enhanced xylose metabolism. Biotechnol. Adv. **doi:**10.1016/j.biotechadv.2013.1003.1004.
14. **Jojima T, Omumasaba CA, Inui M, Yukawa H.** 2010. Sugar transporters in efficient utilization of mixed sugar substrates: current knowledge and outlook. Appl. Microbiol. Biotechnol. **85:**471-480.

15. **Young EM, Comer AD, Huang H, Alper HS.** 2012. A molecular transporter engineering approach to improving xylose catabolism in *Saccharomyces cerevisiae*. Metab. Eng. **14:**401-411.
16. **Shao Z, Zhao H, Zhao H.** 2009. DNA assembler, an *in vivo* genetic method for rapid construction of biochemical pathways. Nucleic Acids Res. **37:**e16.
17. **Rubin-Pitel SB, Zhao H.** 2006. Recent advances in biocatalysis by directed enzyme evolution. Comb. Chem. High T. Scr. **9:**247-257.
18. **Du J, Shao Z, Zhao H.** 2011. Engineering microbial factories for synthesis of value-added products. J. Ind. Microbiol. Biotechnol. **38:**873-890.
19. **Hahn-Hagerdal B, Karhumaa K, Jeppsson M, Gorwa-Grauslund MF.** 2007. Metabolic engineering for pentose utilization in *Saccharomyces cerevisiae*. Adv. Biochem. Eng. Biotechnol. **108:**147-177.
20. **Kim SR, Ha SJ, Wei N, Oh EJ, Jin YS.** 2012. Simultaneous co-fermentation of mixed sugars: a promising strategy for producing cellulosic ethanol. Trends Biotechnol. **30:**274-282.
21. **Roca C, Haack MB, Olsson L.** 2004. Engineering of carbon catabolite repression in recombinant xylose fermenting *Saccharomyces cerevisiae*. Appl. Microbiol. Biotechnol. **63:**578-583.
22. **Du J, Li S, Zhao H.** 2010. Discovery and characterization of novel D-xylose-specific transporters from *Neurospora crassa* and *Pichia stipitis*. Mol. Biosyst. **6:**2150-2156.
23. **Cobb RE, Si T, Zhao H.** 2012. Directed evolution: an evolving and enabling synthetic biology tool. Curr. Opin. Chem. Biol. **16:**285-291.
24. **Cobb RE, Sun N, Zhao H.** 2013. Directed evolution as a powerful synthetic biology tool. Methods **60:**81-90.
25. **Cobb RE, Chao R, Zhao H.** 2013. Directed evolution: past, present and future. AIChE J. **59:**1432-1440.
26. **Bokma E, Koronakis E, Lobedanz S, Hughes C, Koronakis V.** 2006. Directed evolution of a bacterial efflux pump: adaptation of the *E. coli* TolC exit duct to the *Pseudomonas* MexAB translocase. FEBS Lett. **580:**5339-5343.
27. **Foo JL, Leong SS.** 21 May 2013. Directed evolution of an *E. coli* inner membrane transporter for improved efflux of biofuel molecules. Biotechnol. Biofuels **6:**81.
28. **Ren C, Chen T, Zhang J, Liang L, Lin Z.** 2009. An evolved xylose transporter from *Zymomonas mobilis* enhances sugar transport in *Escherichia coli*. Microb. Cell Fact. **8:**66.
29. **Lian J, Ding S, Cai J, Zhang D, Xu Z, Wang X.** 2009. Improving aquaporin Z expression in *Escherichia coli* by fusion partners and subsequent condition optimization. Appl. Microbiol. Biotechnol. **82:**463-470.
30. **Kai L, Kaldenhoff R, Lian J, Zhu X, Dotsch V, Bernhard F, Cen P, Xu Z.** 2010. Preparative scale production of functional mouse aquaporin 4 using different cell-free expression modes. PLoS One **5:**e12972.
31. **Tusnady GE, Simon I.** 2001. The HMMTOP transmembrane topology prediction server. Bioinformatics **17:**849-850.
32. **Spyropoulos IC, Liakopoulos TD, Bagos PG, Hamodrakas SJ.** 2004. TMRPres2D: high quality visual representation of transmembrane protein models. Bioinformatics **20:**3258-3260.

33. **Zhang YH, Lynd LR.** 2005. Cellulose utilization by *Clostridium thermocellum*: bioenergetics and hydrolysis product assimilation. Proc. Natl. Acad. Sci. U. S. A. **102:**7321-7325.
34. **Verduyn C, Postma E, Scheffers WA, van Dijken JP.** 1990. Physiology of *Saccharomyces cerevisiae* in anaerobic glucose-limited chemostat cultures. J. Gen. Microbiol. **136:**395-403.
35. **Gietz RD, Schiestl RH.** 2007. High-efficiency yeast transformation using the LiAc/SS carrier DNA/PEG method. Nat. Protoc. **2:**31-34.

Chapter 3 Reversal of the β-Oxidation Cycles in *Saccharomyces cerevisiae* for the Production of Advanced Biofuels

3.1 Introduction

After decades of intensive research, commercial production of bioethanol has been achieved (1). Due to its intrinsic shortcomings such as low energy density, high corrosivity, and hydroscopicity, ethanol is not compatible with existing fuel distribution infrastructure (2). Thus, increasing effort has been devoted to produce advanced biofuels, such as butanol, long chain alcohols, fatty acid ethyl esters, and alkanes, which have similar properties to current transportation fuels. Notably, most of the "drop-in" fuels are derived from fatty acids (fatty acyl-CoAs or fatty acyl-ACPs), which can be produced by the endogenous fatty acid biosynthetic (FAB) pathways (3). However, the traditional FAB systems suffer from high energy input and complicated regulation, which significantly hinders efficient and cost-effective production of advanced biofuels. Generally, the classic FASs require the consumption of ATP to activate acetyl-CoA to malonyl-CoA and use ACP and NADPH as the co-factors (4, 5). Interestingly, fatty acid degradation pathway or the β-oxidation pathway, which happens in the opposite direction as that of FAB, proceeds in a much more efficient manner. For example, no ATP consuming reaction was involved and CoA and NADH was used instead of ACP and NADPH as the co-factors (6, 7).

To overcome the major limitation of FASs, a recent report demonstrated that the fatty acid degradation enzymes were functional in both degradative and synthetic directions and the *E. coli* β-oxidation cycles could be functionally reversed to synthesize a series of advanced fuels and chemicals, including short, medium, and long chain alcohols and fatty acids (8, 9).

Compared with the traditional engineering strategy, there were several advantages of this novel platform for advanced biofuel production, such as high efficiency by bypassing the energy consuming and rate-limiting step to produce malonyl-CoA and flexibility to engineer the production of fatty alcohols and fatty acids with different chain length.

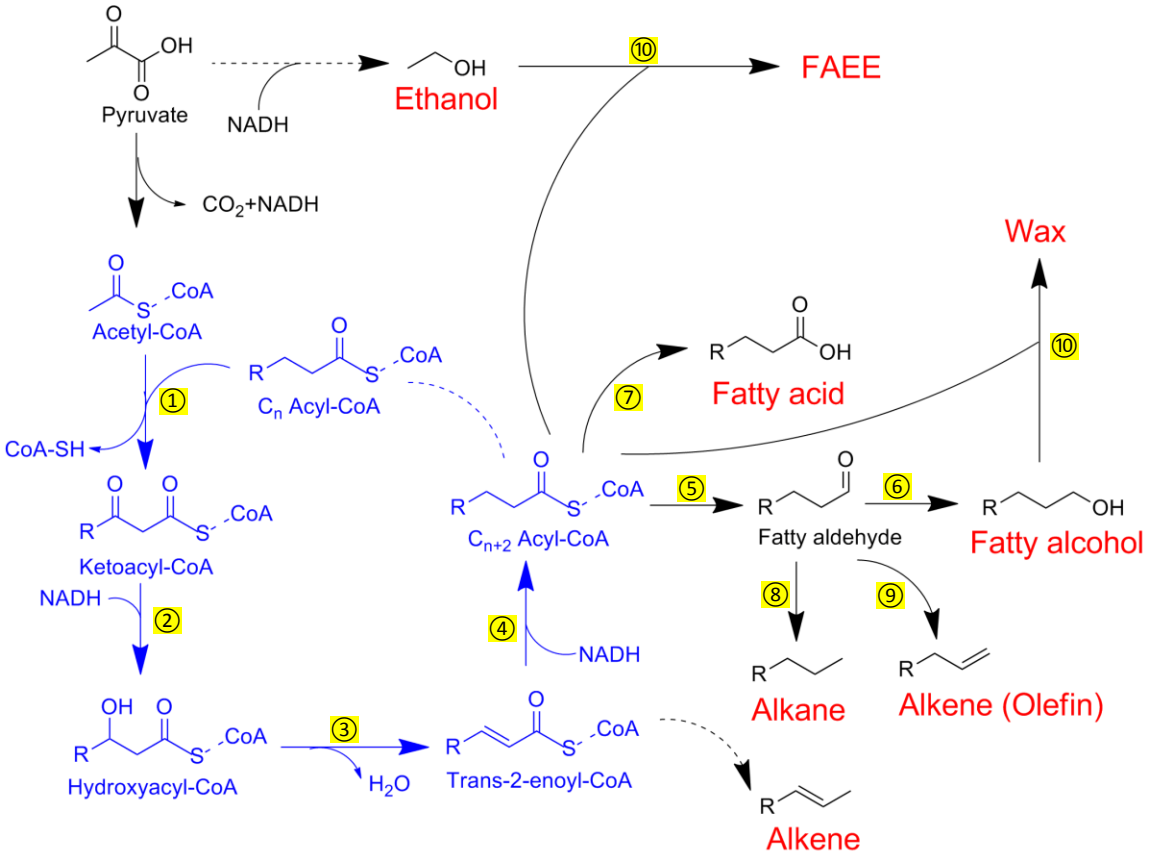

Figure 3.1 Overview of advanced biofuel synthesis by reversing the β-oxidation cycles. ① β-Ketoacyl-CoA Synthase (KS); ② β-Ketoacyl-CoA Reductase (KR); ③ β-Hydroxyacyl-CoA Dehydratase (HTD); ④ Trans-2-Enoyl-CoA Reductase (TER); ⑤ Fatty Acyl-CoA Reductase (FAR); ⑥ Alcohol Dehydrogenase (ADH); ⑦ Thioesterase (TE); ⑧ Aldehyde Decarbonylase; ⑨ Wax Synthase/Diacylglycerol Acyltransferase (WS/DGAT)

Compared with *E. coli*, the currently most popular host for metabolic engineering and synthetic biology studies, *S. cerevisiae* is a more suitable for industrial-scale production of biofuels from lignocellulosic biomass, because of its high tolerance to harsh conditions, the ability of high density fermentation, and free of phage contamination (1, 10). Although the

reversal of β-oxidation for efficient fuel synthesis was demonstrated in *E. coli*, it might be extended to this eukaryotic system as well, owing to the ubiquitous nature of β-oxidation (7, 8). Therefore, we aimed to develop a new platform, based on the reversed β-oxidation pathways, to synthesize efficiently and cost-effectively a series of fuels and chemicals in *S. cerevisiae*, including but not limited to fatty acids, fatty alcohols, FAEEs, alkanes, and even waxes (Figure 3.1). As proof of concept, β-oxidation enzymes were cloned from various species and expressed in *S. cerevisiae* to test the production of butanol, which requires the reversal of only one cycle of β-oxidation. If possible, more metabolic engineering and synthetic biology efforts will be put to extend this platform to produce long chain fatty acid derived advanced biofuels and redirect the flux towards the desired products.

3.2 Results

3.2.1 Construction of Helper Plasmids to Facilitate Gene Cloning and Pathway Assembly

To facilitate gene cloning and pathway assembly, six helper plasmids with the whole promoter or terminator as the homology region between two adjacent cassettes were constructed. As shown in Figure 3.2 and Table 3.1, besides the eGFP cassette (promoter-eGFP-terminator), there was an additional promoter sequence at the 3' end of the terminator in each helper plasmid, serving as the homologous region for pathway assembly. Each eGFP sequence was flanked by a unique *Bam*HI site at 5' end and *Xho*I site at 3' end, which allowed the cloning of desired genes by replacing the eGFP sequence. In addition, unique restriction enzyme sites were also introduced to flank at both ends of each cassette, which conferred the flexibility to remove the whole cassette by restriction digestion.

Table 3.1 Helper plasmids constructed for the reversed β-oxidation pathways

Plasmids	Construct
Helper1	pRS425-*Stu*I-GPM1p-*Bam*HI-eGFP-*Xho*I-ADH1t-*Avr*II
Helper2	pRS425-*Avr*II-ADH1t-GPDp-*Bam*HI-eGFP-*Xho*I-CYC1t-*Sbf*I-ENO2p
Helper3	pRS425-*Sbf*I-ENO2p-*Bam*HI-eGFP-*Xho*I-PGK1t-*Not*I-TPI1p
Helper4	pRS425-*Not*I-TPI1p-*Bam*HI-eGFP-*Xho*I-TPI1t-*Sac*II-TEFK1p
Helper5	pRS425-*Sac*II-TEF1p-*Bam*HI-eGFP-*Xho*I-TEF1t-*Xma*I
Helper6	pRS425-TEF1t-PGK1p-*BamHI*-eGFP-*HindIII*-HXT7t

As shown in Figure 3.2, the whole cassettes together with the downstream homologous sequences were PCR amplified and co-transformed into *S. cerevisiae* to assemble the whole pathway via the DNA assembler method.

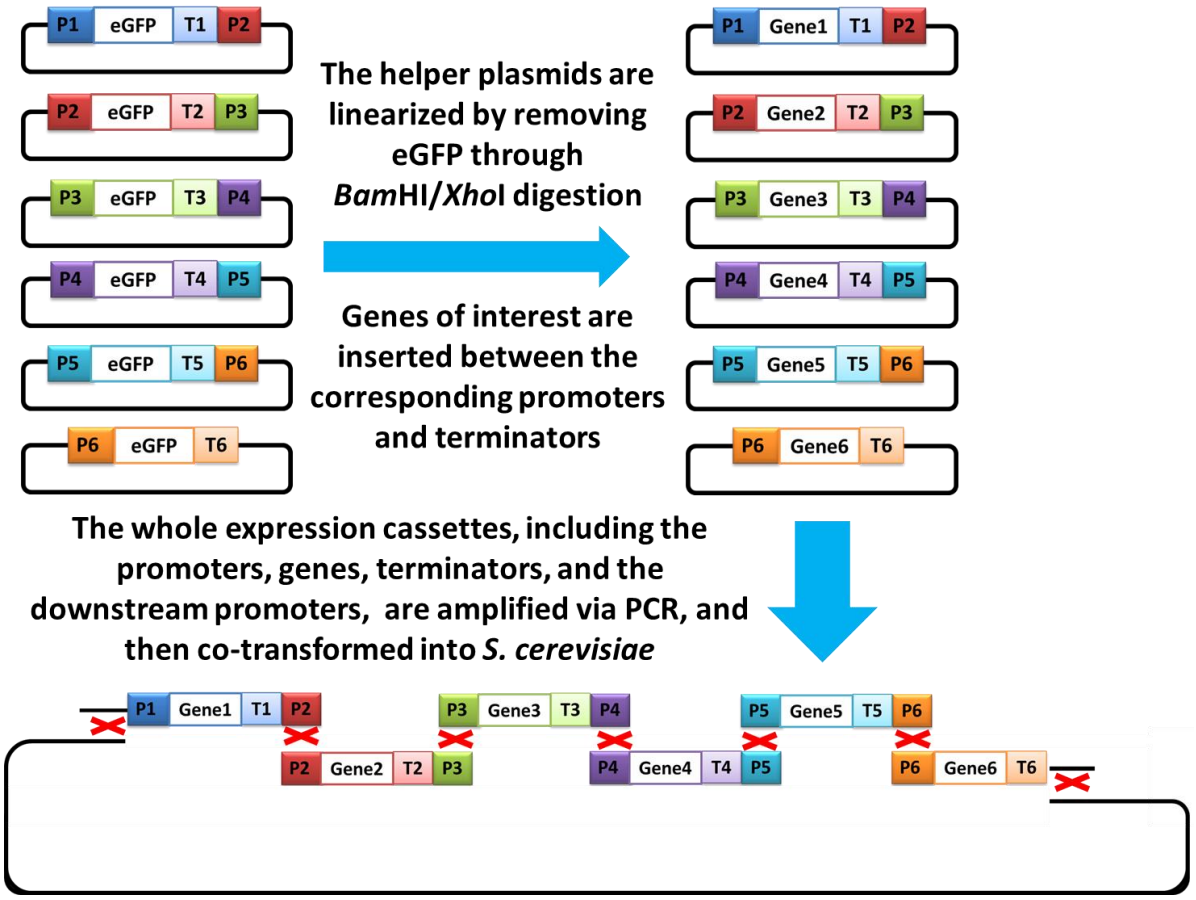

Figure 3.2 Schemes of gene cloning and pathway construction via DNA assembler using the six helper plasmids.

3.2.2 Searching for Functional β-Oxidation Enzymes Expressed in the Cytosol of S. cerevisiae

To test the possibility of the reversal of β-oxidation cycle in *S. cerevisiae*, more than 40 genes from various species were cloned to construct the reversed β-oxidation pathways. Using the *E. coli* pathway as the start point, gene candidates to be cloned followed the following criteria: 1) *E. coli* and yeast β-oxidation enzymes (6, 7, 11, 12); 2) proteins sharing high homology with the *E. coli* reversed β-oxidation pathway (8); 3) putative enzymes that are predictive to have the desired functions. Due to the availability of the CoA substrates, enzyme activity assays were carried out using C_4-CoAs, including acetoacetyl-CoA, β-hydroxybutyryl-CoA, and crotonoyl-CoA (*trans*-2-Butenoyl-CoA). Considering the broad specificity of the β-oxidation enzymes, the performed enzyme assays using C_4-CoAs should be sufficient to represent the β-oxidation activities (13). Since β-oxidation enzymes were localized either in the mitochondrion or the peroxisome in eukaryotes, the targeting sequences were predicted using the on-line tools and removed during cloning in order to be expressed in the cytosol of *S. cerevisiae*.

3.2.2.1 β-Ketoacyl-CoA Synthase (KS)

The β-ketoacyl-CoA synthase activity was carried out in the thiolysis direction using acetoacetyl-CoA as the substrate. As shown in Table 3.2, several KS candidate genes were cloned from both *S. cerevisiae* and *E. coli*. The thiolase from *Clostridium acetobutylicum* (CaThl), which is involved in the fermentative production of butanol (14), was used as the positive control. Both acetyl-transferase (ERG10, EcAtoB and EcYqeF) and acyl-transferase (cytoFOX3 and EcFadA) were included for analysis, which showed short chain specificity (15) and broad specificity (12), respectively.

Table 3.2 β-Ketoacyl-CoA synthases cloned for the reversed β-oxidation pathways

KS	Activity	Comments
Helper1-CaThl	Positive Control	Specific for short chain acyl-CoAs
Helper1-ERG10	Functional	
Helper1-cytoFox3	Functional	Broad specificity
Helper1-EcAtoB	No activity	
Helper1-EcYqeF	No activity	
Helper1-EcFadA	No Activity	

As shown in Figure 3.3, ERG10 showed the highest activity towards acetoacetyl-CoA among all enzymes tested, which was consistent with a previous report that ERG10 was optimal for butanol production in yeast (16). Unfortunately, all the enzymes cloned from *E. coli* are un-functional. By removing the peroxisomal targeting sequences, FOX3 was relocalized to the cytosol and functionally expressed. Although the activity of cytoFOX3 was a bit lower than that of ERG10, this β-oxidation enzyme should show broad specificity towards different chain length substrates. Therefore, cytoFOX3 was chosen to construct the reversed β-oxidation pathways.

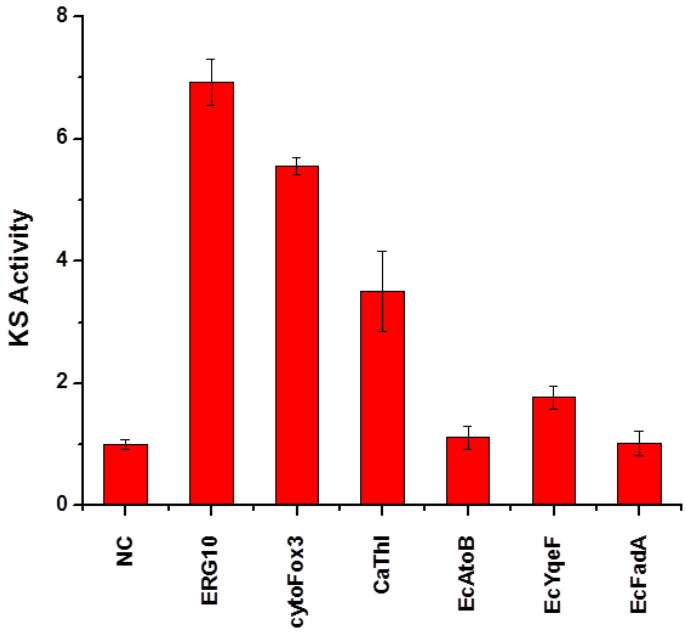

Figure 3.3 KS activity assay using acetoacetyl-CoA as the substrate.

3.2.2.2 Multi-functional Enzyme (KR and HTD)

The second and third steps of β-oxidation were carried out by a multi-functional enzyme, FOX2 in *S. cerevisiae* (12) and FadB in *E. coli* (11). Unfortunately, neither of them could be functionally expressed in the cytosol of *S. cerevisiae*. Therefore, more FOX2 homologs were found by BLAST search and cloned for enzyme activity assay, as listed in Table 3.3.

Table 3.3 Multi-functional enzymes cloned for the reversed β-oxidation pathways. All strains used are all requested from ARS culture collection (NRRL). H8, H10, H15, and H22 failed to be cloned or the strains requested failed to grow

Plasmid	Constructs	Origin
cytoFOX2	Helper2-cytoFOX2	*Saccharomyces cerevisiae*
EcFadB	Helper2-EcFadB	*Escherichia coli*
H1	Helper2-cytoFOX2	*Torulaspora delbrueckii*
H2	Helper2-cytoFOX2	*Candida glabrata*
H3	Helper2-cytoFOX2	*Naumovozyma dairenensis*
H4	Helper2-cytoFOX2	*Vanderwaltozyma polyspora*
H5	Helper2-cytoFOX2	*Naumovozyma castellii*
H6	Helper2-cytoFOX2	*Kluyveromyces lactis*
H7	Helper2-cytoFOX2	*Tetrapisispora phaffii*
H8	Helper2-cytoFOX2	*Lachancea thermotolerans*
H9	Helper2-cytoFOX2	*Zygosaccharomyces rouxii*
H10	Helper2-cytoFOX2	*Eremothecium cymbalariae*
H11	Helper2-cytoFOX2	*Ashbya gossypii*
H12	Helper2-cytoFOX2	*Pichia pastoris*
H13	Helper2-cytoFOX2	*Pichia farinosa*
H14	Helper2-cytoFOX2	*Hansenula polymorpha*
H15	Helper2-cytoFOX2	*Debaryomyces hansenii*
H16	Helper2-cytoFOX2	*Candida parapsilosis*
H17	Helper2-cytoFOX2	*Pichia guilliermondii*
H18	Helper2-cytoFOX2	*Candida dubliniensis*
H19	Helper2-cytoFOX2	*Candida tropicalis*
H20	Helper2-cytoFOX2	*Scheffersomyces stipitis*
H21	Helper2-cytoFOX2	*Lodderomyces elongisporus*
H22	Helper2-cytoFOX2	*Spathaspora passalidarum*
H23	Helper2-cytoFOX2	*Candida tenuis*
H24	Helper2-cytoFOX2	*Yarrowia lipolytica*

Unfortunately, as shown in Table 3.4, although more than 20 candidate enzymes from different species were tested, none was found to possess KR and HTD activities towards acetoacetyl-CoA and crotonoyl-CoA.

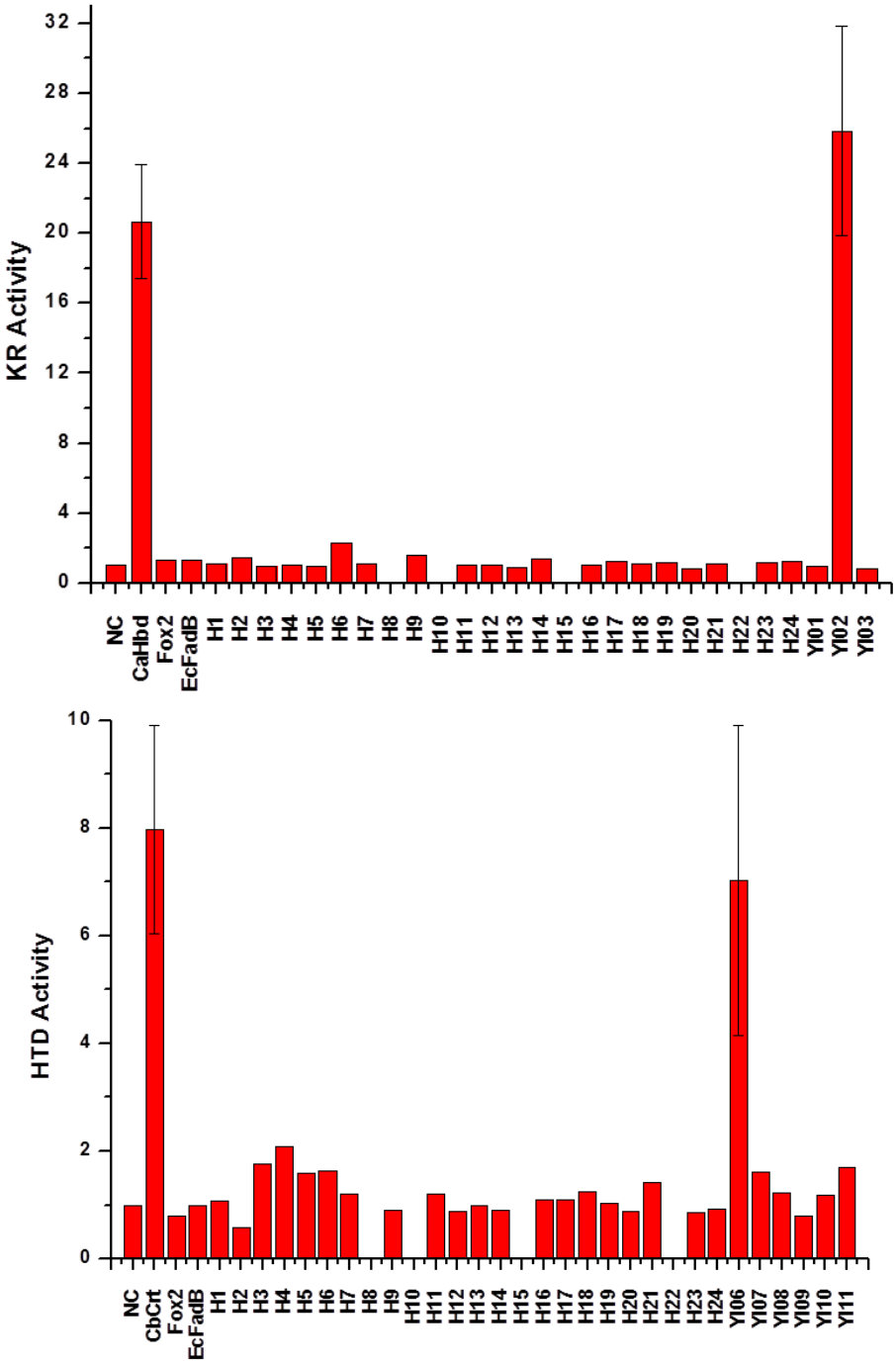

Figure 3.4 HBD and CRT activity assay of the multifunctional enzymes.

There were several explanations for the lack of KR and HTD activities of FOX2 homologs towards acetoacetyl-CoA and crotonoyl-CoA. FOX2 from *S. cerevisiae* was found to have the highest activity towards medium chain and long chain substrates, while the activity towards C_4 compound could be much lower (17). Another explanation could be the different folding environments between cytosol and peroxisome, which might completely abolish their enzymatic activities. To test the possibility of the first hypothesis, FOX2 from *Yarrowia lipolytica* was also included in this study. As oleaginous yeasts can accumulate fatty acids and lipids to high levels (18), it is rational to speculate that they also have a very efficient β-oxidation system. Unfortunately, the *Yarrowia* FOX2 was found to have no enzymatic activity either (Figure 3.4). Therefore, it was concluded that the difference in folding environments between cytosol and peroxisome caused more than 20 FOX2 homologs to be un-functionally expressed in the cytosol of *S. cerevisiae*.

Table 3.4 KRs and HTDs cloned from *Yarrowia lipolytica*

Plasmids	Constructs	Comments
CaHbd	Helper2-CaHbd	Positive control, specific for short chain substrate
Yl01	Helper2-YALI0A02046	
Yl02	Helper2-YALI0C08811	Active KR, broad specificity
Yl03	Helper2-YALI0F29975	
CbCrt	Helper6-CbCrt	Positive control, specific for short chain substrate
Yl06	Helper6-YALI0B10406	Active HTD, broad specificity
Yl07	Helper6-YALI0F22121	
Yl08	Helper6-YALI0D06215	
Yl09	Helper6-YALI0A07733	
Yl10	Helper6-YALI0F28567	
Yl11	Helper6-YALI0D09493	

Different from *S. cerevisiae*, some oleaginous yeasts were found to have another set of β-oxidation system in the mitochondrion (19), besides the traditional system in the peroxisome. Therefore, the mitochondrial β-oxidation enzymes together with some homologs sharing high

homology were cloned from *Y. lipolytica*, and the β-hydroxybutyryl-CoA dehydrogenase from *C. acetobutylium* (CaHbd) and crotonase from *C. beijerinckii* (CbCrt) were included as the positive controls (14, 20) (Table 3.4). Different from the peroxisomal β-oxidation system that a multifunctional enzyme can catalyze the second and third step of β-oxidation, there are two separate enzymes in the mitochondrial system to possess KR and HTD activities, encoded by *YALI0C08811* and *YALI0B10406*, respectively (19). As shown in Figure 3.4, both of the mitochondrial β-oxidation enzymes could be functionally expressed in the cytosol of yeast, both of which showed comparable enzymatic activities with the *Clostridium* equivalents. Thus, these two enzymes were chosen to construct the reversed β-oxidation pathways.

3.2.2.3 *Trans*-2-Enoyl-CoA Reductase (TER)

The first step of β-oxidation was carried out by fatty acid oxidase with the involvement of oxygen molecule, which was the only irreversible step (6, 7, 12). Thus, *trans*-2-Enoyl-CoA reductases (TERs), which are involved in fatty acid biosynthesis (FAB) and only catalyze the reaction in the reducing direction, were chosen to construct the reversed β-oxidation pathways instead of the fatty acid oxidase. In fact, several TERs, such as those from *Euglena gracilis* (EgTer) and *Treponema denticola* (TdTer), have been characterized (21-23) and determined to significantly improve the production of butanol (24, 25) and short chain fatty acids (9) in *E. coli*. Therefore, TERs from *E. coli*, *S. cerevisiae*, *E. gracilis* and *T. denticola* and some homologs that shared high homology were cloned (Table 3.4).

Table 3.5 TERs cloned for the reversed β-oxidation pathways

Plasmids	Comments
Helper3-cytoETR1	Active, involved in the mitochondrial FAB in *S. cerevisiae*
Helper3-ZTA1	
Helper3-cytoSPS19	
Helper3-YNL134C	
Helper3-YLR460C	
Helper3-YCR102C	
Helper3-EcYdiO	
Helper3-EcFabI	Active, involved in FAB in *E. coli*
Helper3-EgTer	Active, involved in the mitochondrial FAB in *Euglena gracilis*
Helper3-TdTer	Active, involved in FAB in *Treponema denticola*

As shown in Figure 3.5, several candidates involved in the biosynthesis of fatty acids, such as the endogenous ETR1, FabI from *E. coli*, TER from *E. gracilis*, and TER from *T. denticola*, were determined to possess the TER activity. Consistent with the previous work (21, 22), TdTer was found to have the highest activity when crotonoyl-CoA was used as the substrate. Therefore, ETR1 and TdTer were chosen to construct the reversed β-oxidation pathways.

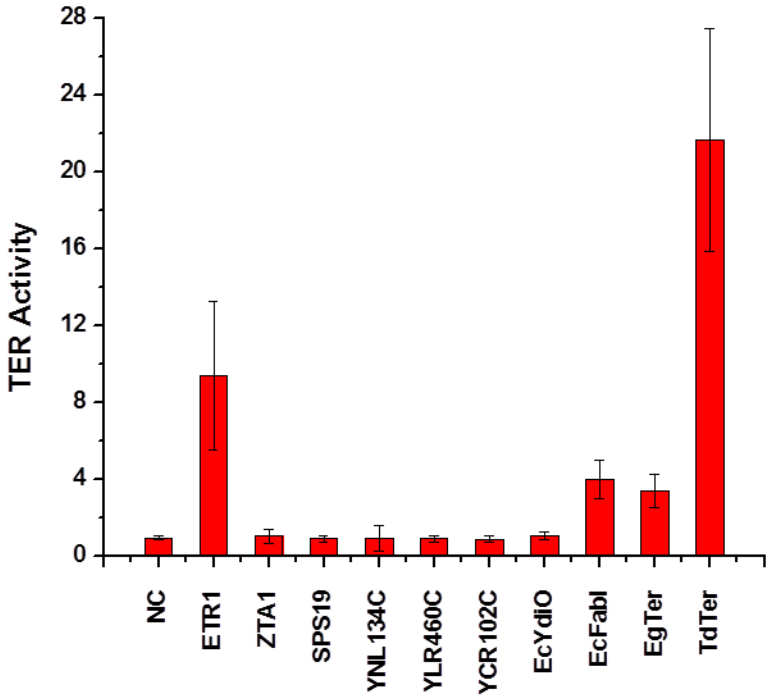

Figure 3.5 TER activity assay using crotonoyl-CoA as the substrate.

3.2.3 Butanol Biosynthesis as Proof-of-concept

After intensive cloning and enzyme activity assays, several candidates were found to be functionally expressed in yeast with the desired activities, with at least one functional enzyme in each step of β-oxidation. Therefore, using the DNA assembler method (26), reversed β-oxidation pathways could be readily constructed. As a proof of concept, butanol biosynthesis that requires only one cycle reversal of β-oxidation was selected. As shown Table 3.6, butanol pathways based on reversed β-oxidation were constructed using ERG10/cytoFOX3-cytoYl02-cytoYl06-TdTer/cytoETR1, based on the enzyme activity assay results. To pull butyryl-CoA to synthesize butanol, the CoA-acylating aldehyde dehydrogenase from *E. coli* (EcEutE) (27, 28) and butanol dehydrogenase from *C. acetobutylium* (CaBdhB) (14) were included in the reversed β-oxidation pathways.

Table 3.6 Reversed β-oxidation pathways constructed for the synthesis of butanol

Pathways	Constructs
BuPa31	pRS426-ERG10-cytoYl02-cytoYl06-TdTer-EcEutE-CaBdhB
BuPa32	pRS426-cytoFOX3-cytoYl02-cytoYl06-TdTer-EcEutE-CaBdhB
BuPa34	pRS426-ERG10-cytoYl02-cytoYl06-cytoETR1-EcEutE-CaBdhB
BuPa35	pRS426-cytoFOX3-cytoYl02-cytoYl06-cytoETR1-EcEutE-CaBdhB
BuPa37	pRS426-ERG10-eGFP-cytoYl06-TdTer-EcEutE-CaBdhB
BuPa38	pRS426-cytoFOX3-eGFP-cytoYl06-TdTer-EcEutE-CaBdhB

As shown in Figure 3.6, butanol, although at very low titer, could be detected using the strains containing the constructed reversed β-oxidation pathways, including BuPa31, BuPa32 BuPa34, and BuPa35. Currently, BuPa34 produced the highest amount of butanol, with a titer of as high as 20 mg/L in the wild-type yeast strain. Although the butanol titer was still rather low compared with that in *Clostridia* (20) and *E. coli* (8, 24, 25), it was approximately 10 fold higher

than a previous report using the *Clostridum* butanol fermentative pathway in yeast (16). This result indicated the high efficiency of the reversed β-oxidation pathways.

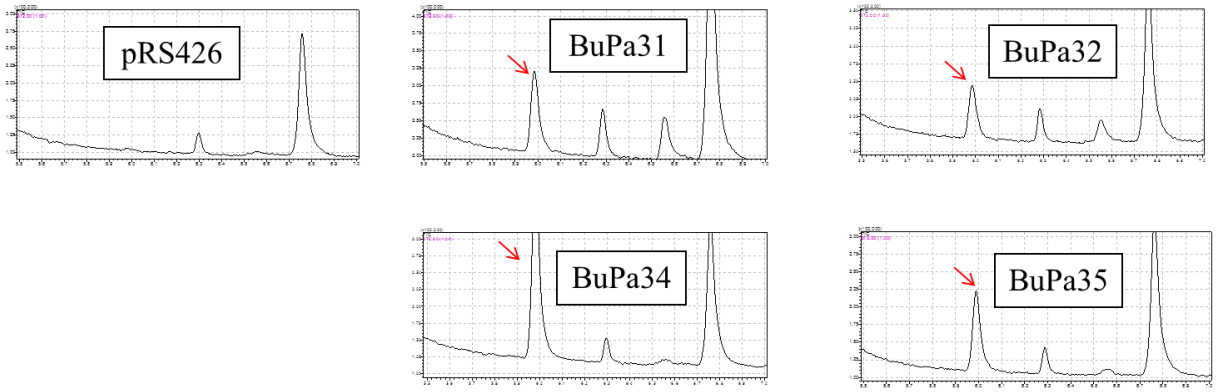

Figure 3.6 Production of butanol by the reversed β-oxidation pathway.

The assembled pathways containing functional β-oxidation enzymes could produce a small amount of butanol, indicating the reversal of β-oxidation cycles. To be 100% sure that the detected butanol was produced via the reversed β-oxidation pathway, pathway deletion and complementation were carried out. Replacing cytoYl02 having KR activity with eGFP, no butanol production was observed, while co-expression of cytoYl02 together with the "deletion pathways" (BuPa37 and BuPa38) could restore the butanol production (Figure 3.7).

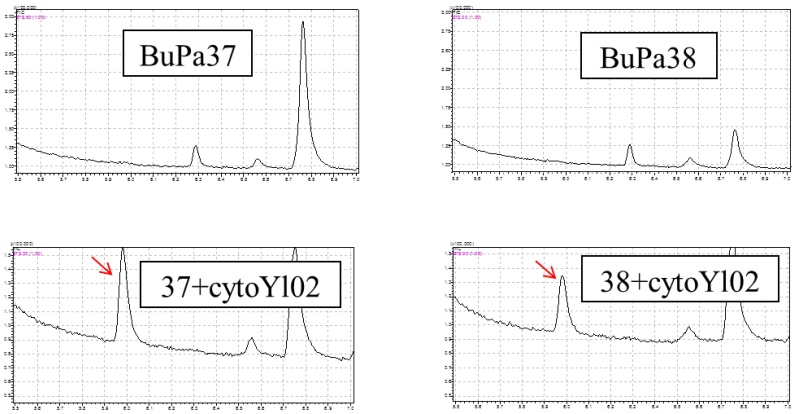

Figure 3.7 Complementation of butanol production by the reversed β-oxidation pathway.

3.3 Discussion

The reversal of β-oxidation was confirmed by butanol production and the next step is to develop this pathway into a platform for synthesis of a wide variety of fatty acid-derived fuels and chemicals. The yeast β-oxidation enzymes show broad specificity towards short-, medium-, and long-chain substrates (6, 7), which promises a versatile platform but also challenges the control of the chain length of the final products. Currently, the chain length of the products was mainly controlled by the specificity of the terminal enzymes. If necessary, protein engineering will be carried out to engineer the terminal enzymes with desired properties. An alternative method to control the chain length of the major products is to use the animal β-oxidation system. Different from the case in yeast and fungi, fatty acids are degraded to medium chain acyl-CoA (C_6-C_{10}) in the peroxisome and then completely degraded into acetyl-CoA in the mitochondria (29). Therefore, by reversal of the animal mitochondria β-oxidation cycle, fuels and chemicals with medium chain length will be the major products.

Since *S. cerevisiae* is a natural host to produce ethanol and fatty acyl-CoA is produced by the reversed pathway, overexpression of additional one single protein, WS/DGAT, is sufficient to synthesize FAEE in the engineered yeast strain (Figure 3.1) (30). On the contrary, the product of the traditional FAB pathway is acyl-ACP, which should be thiolysed to release free fatty acid by thioesterase (TE) and then converted to acyl-CoA by fatty acyl-CoA synthase (FAA) (31). Therefore, besides the high efficiency of the reversed β-oxidation pathway, another advantage of such system is the decreased biosynthetic steps for FAEE production.

The high efficiency of the reversed β-oxidation pathway was characterized by its energetic benefits of the malonyl-CoA independence and the use of CoA and NADH instead of ACP and NADPH as the cofactors (8). However, compared with the high efficiency of the

reversed β-oxidation pathway in *E. coli*, this system seemed to not work very well in yeast, as shown by the relative low butanol productivity. One explanation for this discrepancy is the difference in acetyl-CoA biosynthesis. In *E. coli*, acetyl-CoA is steadily synthesized from pyruvate by either pyruvate dehydrogenase (PDH) under aerobic conditions (32) and pyruvate-formate lyase (PFL) under anaerobic conditions (33). While in *S. cerevisiae*, acetyl-CoA is mainly generated in the mitochondria, and the reversed β-oxidation pathway enzymes are localized in the cytosol. What's worse, *S. cerevisiae* lacks the machinery to export the mitochondrial acetyl-CoA to the cytosol (34). Thus, there is not enough substrate for the reversed β-oxidation pathway, due to the compartmentalization of acetyl-CoA metabolism. In *S. cerevisiae*, the cytosolic acetyl-CoA is generated via the PDH-bypass pathway, from pyruvate to acetaldehyde and then to acetate, which is activated to acetyl-CoA by the acetyl-CoA synthase (ACS) at the cost of two ATP molecules (35). The activation of acetate is the rate-limiting step in cytosolic acetyl-CoA synthesis, resulting from the low activity of ACS and high energy input. Several metabolic engineering strategies have been carried out to boost the availability of acetyl-CoA in yeast, such as the use of an ACS mutant which showed much higher activity (36-39) and the introduction of heterologous acetyl-CoA biosynthetic pathways with less energy input (40, 41). Notably, these strategies have been applied to improve the production of isoprenoids (36), polyhydroxybutyrate (38, 40), butanol (39), fatty acids (41), and α-santalene (37) in *S. cerevisiae*. Therefore, the construction of an acetyl-CoA overproducing yeast may significantly enhance the efficiency of the reversed β-oxidation pathway for advanced biofuel synthesis.

3.4 Conclusions and Future Plans

To construct a functional reversed β-oxidation pathway, approximately 50 enzyme homologs were cloned from various species. Based on the enzyme activity assays, at least one functional enzyme was obtained for each catalytic step. To demonstrate the proof of concept, butanol biosynthesis that requires only one cycle reversal of β-oxidation was selected. The production of a small amount of butanol indicated a functionally reversed β-oxidation pathway. Future work will focus on metabolic engineering strategies to increase the intracellular acetyl-CoA level to further increase the titer and productivity of butanol and expand this platform to synthesize advanced fuel molecules with longer carbon chains.

3.5 Materials and Methods

3.5.1. Strains, Media, and Cultivation Conditions

E. coli strain DH5α (Cell Media Facility, University of Illinois at Urbana Champaign) was used to maintain and amplify plasmids. *S. cerevisiae* CEN.PK2-1C (*MATa ura3-52 trp1-289 leu2-3,112 his3Δ1 MAL2-8^{C} SUC2*, EUROSCARF) was used as the host for homologous recombination based cloning and butanol fermentation. Yeast strains were cultivated in complex medium consisting of 2% peptone and 1% yeast extract supplemented with either 2% glucose (YPD). Recombinant strains were grown on synthetic complete medium consisting of 0.17% yeast nitrogen base, 0.5% ammonium sulfate, and 0.07% amino acid drop out mix without leucine or uracil (MP Biomedicals, Solon, OH), supplemented with 2% glucose (SCD-Leu or SCD-Ura). *E. coli* strains were cultured at 37^{o}C in Luria-Bertani broth containing 100 μg/mL ampicillin. *S. cerevisiae* strains were cultured at 30^{o}C and 250 rpm for aerobic growth, and 30^{o}C

and 100 rpm in un-baffled shaker flasks for oxygen limited fermentation. All restriction enzymes, Q5 High Fidelity DNA polymerase, and the *E. coli* - *S. cerevisiae* shuttle vectors, including pRS425 and pRS426, were purchased from New England Biolabs (Ipswich, MA). All chemicals were purchased from either Sigma-Aldrich or Fisher Scientific.

3.5.2 DNA Manipulation

The yeast homologous recombination based DNA assembler method (26) was used to construct the helper plasmids, clone candidate genes and assemble the reversed β-oxidation pathways. Briefly, polymerase chain reaction (PCR) was used to generate DNA fragments with homology arms at both ends, which were purified with a QIAquick Gel Extraction Kit (Qiagen, Valencia, CA) and co-transformed along with the linearized backbone into *S. cerevisiae*. All genetic elements, including promoters, coding sequences, and terminators, were PCR-amplified from their corresponding genomic DNAs. Wizard Genomic DNA Purification Kit (Promega, Madison, WI) was used to extract the genomic DNAs from both bacteria and yeasts, according to the manufacturer's protocol. To confirm the correct clones, yeast plasmids were isolated using a Zymoprep Yeast Plasmid Miniprep II Kit (Zymo Research, Irvine, CA) and re-transformed into *E. coli* DH5α competent cells. Plasmids were isolated using a QIAprep Spin Miniprep Kit (Qiagen) and confirmed using both diagnostic PCRs and restriction digestions. Yeast strains were transformed using the LiAc/SS carrier DNA/PEG (42) method, and transformants were selected on either SCD-Leu or SCD-Ura plates.

3.5.3 Enzyme Activity Assays

To measure the activity of enzymes expressed in yeast, a single colony was inoculated into 5 mL of SCD-Leu medium, and cultured under aerobic conditions for about 36 h. Then cells were collected by centrifugation at 4,000 *g* for 5 min at 4^{o}C, washed twice with pre-chilled water, and resuspended in 250 μL Yeast Protein Extraction Reagent (YPER). After incubation at 25^{o}C with 700 rpm shaking in a thermomixer for 20 minutes, the supernatant containing all soluble proteins were separated by centrifugation at 14,000g for 10 min at 4^{o}C and ready for enzyme activity assays. All the assays were performed in 96-well microplates at 30^{o}C and the spectrophotometric changes were monitored using the Biotek Synergy 2 Multi-Mode Microplate Reader (Winooski, VT). The reaction was initiated by the addition of 20-40 μL cell extract, to a total volume of 200 μL. Enzyme activity was calculated using the initial reaction rate and normalized to the total protein concentration determined by the Bradford assay.

The KS activity was measured by monitoring the disappearance of acetoacetyl-CoA, corresponding to the thiolysis direction of the enzymatic reaction, which was monitored by the decrease in absorbance at 303 nm. The reaction mixture contained 100 mM Tris-HCl (pH 8.0), 10 mM $MgSO_4$, 200 μM acetoacetyl-CoA, and 200 μM CoA.

The KR activity was measured by monitoring the decrease of absorption at 340 nm, corresponding to consumption of NADH in the reducing direction of the reaction. The reaction mixture contained 100 mM potassium phosphate buffer (pH 7.3), 200 μM NADH, and 200 μM acetoacetyl-CoA.

The HTD activity was measured by the decrease of absorption at 263nm, corresponding to disruption of the carbon-carbon double bond of crotonoyl-CoA. The assay mixture contained 100 mM Tris-HCl (pH 7.6) and 100 μM crotonoyl-CoA.

The TER activity was measured at 340 nm, corresponding to consumption of NADH to reduce crotonoyl-CoA. The reaction mixture contained 100 mM potassium phosphate buffer (pH 6.2), 200 μM NADH, and 200 μM crotonoyl-CoA.

3.5.4 Butanol Fermentation and Detection

A single colony with the reversed β-oxidation pathway from the newly transformed plate was inoculated into 3 mL SCD-Ura medium, and cultured under aerobic conditions for 36 h. Then 200 μL seed culture was transferred into 10 mL fresh SCD-Ura medium in a 50 mL unbaffled shaker flask at an initial OD_{600} of about 0.05, and cultured under oxygen-limited conditions for butanol fermentation. Samples were taken every 12 h after inoculation until no further increase in butanol production was observed.

Samples were centrifuged at 14,000 rpm for 10 min and the resulting supernatant was analyzed by a Shimadzu GCMS-QP2010 Plus GC-MS equipped with an AOC-20i+s autosampler and a DB-Wax column with a 0.25 μm film thickness, 0.25 mm diameter, and 30 m length (Agilent Inc., Palo Alto, CA). Injection port and interface temperature was set at 250 ℃, and the ion source set to 230 ℃. The helium carrier gas was set at a constant flow rate of 2 mL/min. The oven temperature program was set as the following: a) 3 min isothermal heating at 50 ℃, b) increase at the rate of 15 ℃ min^{-1} to 120 ℃, c) increase at the rate of 50 ℃ min^{-1} to 230 ℃, d) and then isothermal heating at 230 ℃ for additional 2.5 min. The mass spectrometer was

operated with a solvent cut time of 1.5 min, an event time of 0.2 s, a scan speed of 2500 from the range of 30-500 mass to charge (m/z) ratio. Concentrations were determined by the standard curve methods, with 50 mg/L methanol as the internal standard.

3.5.5 Prediction of the Mitochondrial and Peroxisomal Targeting Sequences

The mitochondrial targeting sequences of the candidate proteins were predicted using the MITOPROT online tool (http://ihg.gsf.de/ihg/mitoprot.html) (43). The peroxisomal targeting sequences were predicted using the PTSs predictor from PeroxisomeDB 2.0 (http://www.peroxisomedb.org/Target_signal.php) (44).

3.6 References

1. **Hong KK, Nielsen J.** 2012. Metabolic engineering of *Saccharomyces cerevisiae*: a key cell factory platform for future biorefineries. Cell Mol. Life Sci. **69:**2671-2690.
2. **Zhang F, Rodriguez S, Keasling JD.** 2011. Metabolic engineering of microbial pathways for advanced biofuels production. Curr. Opin. Biotechnol. **22:**775-783.
3. **Handke P, Lynch SA, Gill RT.** 2011. Application and engineering of fatty acid biosynthesis in *Escherichia coli* for advanced fuels and chemicals. Metab. Eng. **13:**28-37.
4. **Chan DI, Vogel HJ.** 2010. Current understanding of fatty acid biosynthesis and the acyl carrier protein. Biochem. J. **430:**1-19.
5. **Lennen RM, Pfleger BF.** 2012. Engineering *Escherichia coli* to synthesize free fatty acids. Trends Biotechnol. **30:**659-667.
6. **van Roermund CW, Waterham HR, Ijlst L, Wanders RJ.** 2003. Fatty acid metabolism in *Saccharomyces cerevisiae*. Cell Mol. Life Sci. **60:**1838-1851.
7. **Trotter PJ.** 2001. The genetics of fatty acid metabolism in *Saccharomyces cerevisiae*. Annu. Rev. Nutr. **21:**97-119.
8. **Dellomonaco C, Clomburg JM, Miller EN, Gonzalez R.** 2011. Engineered reversal of the beta-oxidation cycle for the synthesis of fuels and chemicals. Nature **476:**355-359.
9. **Clomburg JM, Vick JE, Blankschien MD, Rodriguez-Moya M, Gonzalez R.** 2012. A synthetic biology approach to engineer a functional reversal of the beta-oxidation cycle. ACS Synth. Biol. **1:**541-554.
10. **Du J, Shao Z, Zhao H.** 2011. Engineering microbial factories for synthesis of value-added products. J. Ind. Microbiol. Biotechnol. **38:**873-890.

11. **Campbell JW, Morgan-Kiss RM, Cronan JE.** 2003. A new *Escherichia coli* metabolic competency: growth on fatty acids by a novel anaerobic beta-oxidation pathway. Mol. Microbiol. **47:**793-805.
12. **Hiltunen JK, Mursula AM, Rottensteiner H, Wierenga RK, Kastaniotis AJ, Gurvitz A.** 2003. The biochemistry of peroxisomal beta-oxidation in the yeast *Saccharomyces cerevisiae*. FEMS Microbiol. Rev. **27:**35-64.
13. **Poirier Y, Antonenkov VD, Glumoff T, Hiltunen JK.** 2006. Peroxisomal beta-oxidation--a metabolic pathway with multiple functions. Biochim. Biophys. Acta **1763:**1413-1426.
14. **Lutke-Eversloh T, Bahl H.** 2011. Metabolic engineering of *Clostridium acetobutylicum*: recent advances to improve butanol production. Curr. Opin. Biotechnol. **22:**634-647.
15. **Hiser L, Basson ME, Rine J.** 1994. ERG10 from *Saccharomyces cerevisiae* encodes acetoacetyl-CoA thiolase. J. Biol. Chem. **269:**31383-31389.
16. **Steen EJ, Chan R, Prasad N, Myers S, Petzold CJ, Redding A, Ouellet M, Keasling JD.** 2008. Metabolic engineering of *Saccharomyces cerevisiae* for the production of *n*-butanol. Microb. Cell Fact. **7:**36.
17. **Qin YM, Marttila MS, Haapalainen AM, Siivari KM, Glumoff T, Hiltunen JK.** 1999. Yeast peroxisomal multifunctional enzyme: (3*R*)-hydroxyacyl-CoA dehydrogenase domains A and B are required for optimal growth on oleic acid. J. Biol. Chem. **274:**28619-28625.
18. **Beopoulos A, Cescut J, Haddouche R, Uribelarrea JL, Molina-Jouve C, Nicaud JM.** 2009. *Yarrowia lipolytica* as a model for bio-oil production. Prog. Lipid Res. **48:**375-387.
19. **Vorapreeda T, Thammarongtham C, Cheevadhanarak S, Laoteng K.** 2012. Alternative routes of acetyl-CoA synthesis identified by comparative genomic analysis: involvement in the lipid production of oleaginous yeast and fungi. Microbiology **158:**217-228.
20. **Lee SY, Park JH, Jang SH, Nielsen LK, Kim J, Jung KS.** 2008. Fermentative butanol production by Clostridia. Biotechnol. Bioeng. **101:**209-228.
21. **Tucci S, Martin W.** 2007. A novel prokaryotic trans-2-enoyl-CoA reductase from the spirochete *Treponema denticola*. FEBS Lett. **581:**1561-1566.
22. **Bond-Watts BB, Weeks AM, Chang MC.** 2012. Biochemical and structural characterization of the trans-enoyl-CoA reductase from *Treponema denticola*. Biochemistry **51:**6827-6837.
23. **Hoffmeister M, Piotrowski M, Nowitzki U, Martin W.** 2005. Mitochondrial *trans*-2-enoyl-CoA reductase of wax ester fermentation from *Euglena gracilis* defines a new family of enzymes involved in lipid synthesis. J. Biol. Chem. **280:**4329-4338.
24. **Bond-Watts BB, Bellerose RJ, Chang MCY.** 2011. Enzyme mechanism as a kinetic control element for designing synthetic biofuel pathways. Nat. Chem. Biol. **7:**222-227.
25. **Shen CR, Lan EI, Dekishima Y, Baez A, Cho KM, Liao JC.** 2011. Driving forces enable high-titer anaerobic 1-butanol synthesis in *Escherichia coli*. Appl. Environ. Microb. **77:**2905-2915.
26. **Shao Z, Zhao H, Zhao H.** 2009. DNA assembler, an *in vivo* genetic method for rapid construction of biochemical pathways. Nucleic Acids Res. **37:**e16.
27. **Roof DM, Roth JR.** 1988. Ethanolamine utilization in *Salmonella typhimurium*. J. Bacteriol. **170:**3855-3863.

28. **Toth J, Ismaiel AA, Chen JS.** 1999. The ald gene, encoding a coenzyme A-acylating aldehyde dehydrogenase, distinguishes *Clostridium beijerinckii* and two other solvent-producing clostridia from *Clostridium acetobutylicum*. Appl. Environ. Microbiol. **65:**4973-4980.
29. **Houten SM, Wanders RJ.** 2010. A general introduction to the biochemistry of mitochondrial fatty acid beta-oxidation. J. Inherit. Metab. Dis. **33:**469-477.
30. **Shi S, Valle-Rodriguez JQ, Khoomrung S, Siewers V, Nielsen J.** 2012. Functional expression and characterization of five wax ester synthases in *Saccharomyces cerevisiae* and their utility for biodiesel production. Biotechnol. Biofuels **5:**7.
31. **Steen EJ, Kang Y, Bokinsky G, Hu Z, Schirmer A, McClure A, Del Cardayre SB, Keasling JD.** 2010. Microbial production of fatty-acid-derived fuels and chemicals from plant biomass. Nature **463:**559-562.
32. **Guest JR, Angier SJ, Russell GC.** 1989. Structure, expression, and protein engineering of the pyruvate dehydrogenase complex of *Escherichia coli*. Ann. N. Y. Acad. Sci. **573:**76-99.
33. **Knappe J, Sawers G.** 1990. A radical-chemical route to acetyl-CoA: the anaerobically induced pyruvate formate-lyase system of *Escherichia coli*. FEMS Microbiol. Rev. **6:**383-398.
34. **Strijbis K, Distel B.** 2010. Intracellular acetyl unit transport in fungal carbon metabolism. Eukaryot. Cell **9:**1809-1815.
35. **Starai VJ, Escalante-Semerena JC.** 2004. Acetyl-coenzyme A synthetase (AMP forming). Cell Mol. Life Sci. **61:**2020-2030.
36. **Shiba Y, Paradise EM, Kirby J, Ro DK, Keasling JD.** 2007. Engineering of the pyruvate dehydrogenase bypass in *Saccharomyces cerevisiae* for high-level production of isoprenoids. Metab. Eng. **9:**160-168.
37. **Chen Y, Daviet L, Schalk M, Siewers V, Nielsen J.** 2013. Establishing a platform cell factory through engineering of yeast acetyl-CoA metabolism. Metab. Eng. **15:**48-54.
38. **Kocharin K, Chen Y, Siewers V, Nielsen J.** 2012. Engineering of acetyl-CoA metabolism for the improved production of polyhydroxybutyrate in *Saccharomyces cerevisiae*. AMB Express **2:**52.
39. **Krivoruchko A, Serrano-Amatriain C, Chen Y, Siewers V, Nielsen J.** 2013. Improving biobutanol production in engineered *Saccharomyces cerevisiae* by manipulation of acetyl-CoA metabolism. J. Ind. Microbiol. Biotechnol. **40:**1051-1056.
40. **Kocharin K, Siewers V, Nielsen J.** 2013. Improved polyhydroxybutyrate production by *Saccharomyces cerevisiae* through the use of the phosphoketolase pathway. Biotechnol. Bioeng. **110:**2216-2224.
41. **Tang X, Feng H, Chen WN.** 2013. Metabolic engineering for enhanced fatty acids synthesis in *Saccharomyces cerevisiae*. Metab. Eng. **16:**95-102.
42. **Gietz RD, Schiestl RH.** 2007. High-efficiency yeast transformation using the LiAc/SS carrier DNA/PEG method. Nat. Protoc. **2:**31-34.
43. **Claros MG, Vincens P.** 1996. Computational method to predict mitochondrially imported proteins and their targeting sequences. Euro. J. Biochem. **241:**779-786.
44. **Schluter A, Real-Chicharro A, Gabaldon T, Sanchez-Jimenez F, Pujol A.** 2010. PeroxisomeDB 2.0: an integrative view of the global peroxisomal metabolome. Nucleic Acids Res. **38:**D800-D805.

Appendix List of Primers used in this thesis.

Primer	Sequence (5'-->3')	Application
oJL0099	gtttcatttttcttgttctattacaac	Clone CDTs
oJL0100	ctattattttagcgtaaaggatgggg	
oJL0101	atgtcgtctcacggctcccatgacggggcc	CDTs confirmation
oJL0102	ctaagcaacgatagcttcggacacatggcc	
oJL0103	atggctcacagcataaacgaaaaggaggcc	
oJL0104	ctaaattgtaactttctcgtcatccggcgc	
oJL0105	atgggcatcttcaacaagaagcccgtggct	
oJL0106	tcaagcaacagacttgccctcatgctcgtg	
oJL0141	attagaaagaaagcatagcaatctaatctaagttttaattacaaaatgggcatcttcaac	CDT2 engineering
oJL0142	gagaaaagaaaaaaattgatctatcgatttcaattcaattcaattcaagcaacagacttg	
oJL0144	caaggcgggaatgcgccatgaccag	Construct point mutations of CDT2 (WT, Q, F, N, QF, QN, FN, and QFN)
oJL0146	gatgatggcgttgccggaccattgg	
oJL0147	tcaacaacgactggtcatggcgcattcccgccttgctccatgctttcccctccatcattc	
oJL0149	aacgactggtcatggcgcattcccgccttgctccaggctatcccctccatcattcagctc	
oJL0151	gtgggttcccgagtctccccgtttc	
oJL0154	gaacagctcctcgcccttgctcaccatactaccactaccagcaacagacttgccctcatg	Construct CDT2-eGFP
oJL0155	attcacgagcatgagggcaagtctgttgctggtagtggtagtatggtgagcaagggcgag	
oJL0201	gcgcgcgtaatacgactcactatagggcgaattgaggcctcatgcgactgggtgagcata	Construction of Helper1 (pRS425-GPM1p-eGFP-ADH1t-PYK1p)
oJL0202	ccccggtgaacagctcctcgcccttgctcaccatggatcctttgattgatttgactgtgt	
oJL0203	cctcacgcaaaataacacagtcaaatcaatcaaaggatccatggtgagcaagggcgagga	
oJL0204	cttgaccaaacctctggcgaagaagtccaaagctctcgagttacttgtacagctcgtcca	
oJL0205	gatcactctcggcatggacgagctgtacaagtaactcgagagctttggacttcttcgcca	
oJL0206	ttgtactgagattaatctccaaaatagtagcattcctaggcatgccggtagaggtgtggt	
oJL0207	ggtcgctcttattgaccacacctctaccggcatgcctaggaatgctactattttggagat	
oJL0208	caagcgcgcaattaaccctcactaaagggaacaaaagctgtgtgatgatgttttatttgt	
oJL0437	agcgcgcgtaatacgactcactatagggcgaattgaggccttagtcgtgcaatgtatgac	
oJL0438	ccccggtgaacagctcctcgcccttgctcaccatggatcctattgtaatatgtgtgtttg	
oJL0209	gcgcgcgtaatacgactcactatagggcgaattgcctaggaatgctactattttggagat	Construction of Helper2 (pRS425-ADH1t-GPDp-eGFP-CYC1t-ENO2p)
oJL0210	ccccggtgaacagctcctcgcccttgctcaccatggatcctgtgatgatgttttatttgt	
oJL0211	agacaccaatcaaaacaaataaaacatcatcacaggatccatggtgagcaagggcgagga	
oJL0212	gtgaatgtaagcgtgacataactaattacatgatctcgagttacttgtacagctcgtcca	
oJL0213	gatcactctcggcatggacgagctgtacaagtaactcgagatcatgtaattagttatgtc	
oJL0214	aagaaccctttctatacccgcagcgtcgacaccctgcagggcaaattaaagccttcgagc	
oJL0215	aggttttgggacgctcgaaggctttaatttgccctgcagggtgtcgacgctgcgggtata	
oJL0216	caagcgcgcaattaaccctcactaaagggaacaaaagctgtattattgtatgttatagta	
oJL0361	gcgcgcgtaatacgactcactatagggcgaattgcctagg agctttggacttcttcgcca	
oJL0362	ccccggtgaacagctcctcgcccttgctcaccatggatccatccgtcgaaactaagttct	
oJL0217	gcgcgtaatacgactcactatagggcgaattgcctgcagggtgtcgacgctgcgggtata	Construction of Helper3 (pRS425-ENO2p-eGFP-PGK1t-TPI1p)
oJL0218	ccccggtgaacagctcctcgcccttgctcaccatggatcctattattgtatgttatagta	
oJL0219	caccaagcaactaatactataacatacaataataggatccatggtgagcaagggcgagga	
oJL0220	aaaaattgatctatcgatttcaattcaattcaatctcgagttacttgtacagctcgtcca	
oJL0221	gatcactctcggcatggacgagctgtacaagtaactcgagattgaattgaattgaaatcg	
oJL0222	tcttccaccaacctgatgggttcctagatatagcggccgccaggaagaatacactatact	
oJL0223	ctctttagatccagtatagtgtattcttcctggcggccgctatatctaggaacccatcag	
oJL0224	caagcgcgcaattaaccctcactaaagggaacaaaagctgttttagtttatgtatgtgtt	

oJL0225	gcgcgtaatacgactcactatagggcgaattggcggccgctatatctaggaacccatcag	Construction of Helper4 (pRS425-TPI1p-eGFP-TPI1t-TEF1p)
oJL0226	ccccggtgaacagctcctcgcccttgctcaccatggatccttttagtttatgtatgtgtt	
oJL0227	ctataactacaaaaaacacatacataaactaaaaggatccatggtgagcaagggcgagga	
oJL0228	aagaagataatatttttatataattatattaatcctcgagttacttgtacagctcgtcca	
oJL0229	gatcactctcggcatggacgagctgtacaagtaactcgaggattaatataattatataaa	
oJL0230	gagtaaaaaaggagtagaaacattttgaagctatccgcggtatataacagttgaaatttg	
oJL0231	aagatgttcttatccaaatttcaactgttatataccgcggatagcttcaaaatgtttcta	
oJL0232	caagcgcgcaattaaccctcactaaagggaacaaaagctgtttgtaattaaaacttagat	
oJL0233	gcgcgcgtaatacgactcactatagggcgaattgccgcggatagcttcaaaatgtttcta	Construction of Helper5 (pRS425-TEF1p-eGFP-TEF1t)
oJL0234	ccccggtgaacagctcctcgcccttgctcaccatggatcctttgtaattaaaacttagat	
oJL0235	agcatagcaatctaatctaagttttaattacaaaggatccatggtgagcaagggcgagga	
oJL0236	aagatatgcaactagaaaagtcttatcaatctccctcgagttacttgtacagctcgtcca	
oJL0237	gatcactctcggcatggacgagctgtacaagtaactcgagggagattgataagacttttc	
oJL0238	cgcaattaaccctcactaaagggaacaaaagctgcccgggatagcgccgatcaaagtatt	
oJL0421	cagtgagcgcgcgtaatacgactcactatagggcgaattgggagattgataagacttttc	Construct Helper6 (pRS425-TEF1t-PGK1p-eGFP-Hxt7t)
oJL0422	ttagagcgtgatcatgaattaataaaagtgttcgcaaaggatcctgttttatatttgttg	
oJL0423	attatctacttttttacaacaaatataaaacaggatcctttgcgaacacttttattaattc	
oJL0424	taggcaccccaggctttacactttatgcttccggctcctatgttgtgtggaattgtgagc	
oJL0671	aagtaattatctacttttttacaacaaatataaaacaggatccatggtgagcaagggcgag	
oJL0672	ttaataaaagtgttcgcaaaaagcttttacttgtacagctcgtccatgccgagagtgatc	
oJL0475	ggttgagtgttgttccagtttggaacaagagtc	Amply Helper1 Cassette
oJL0478	catgccggtagaggtgtggtcaataagag	
oJL0481	agctttggacttcttcgccagaggtttg	Amply Helper2 Cassette
oJL0482	gcttggtgccacttgtcacatacaattc	
oJL0483	cctgcagggtgtcgacgctgcgggtatagaaag	Amply Helper3 Cassette
oJL0484	gtatgtgtttttgtagttatagatttaagcaag	
oJL0487	gcggccgctatatctaggaacccatcaggttg	Amply Helper4 Cassette
oJL0488	gattgctatgctttctttctaatgagcaagaag	
oJL0489	ccgcggatagcttcaaaatgtttctactc	Amply Helper5 Cassette
oJL0490	gcgccgatcaaagtatttgttacgacaatatc	
oJL0491	ggagattgataagacttttctagttgc	Amply Helper6 Cassette
oJL0492	gggtttcgccacctctgacttgagcgtc	
oJL0239	tcataacctcacgcaaaataacacagtcaaatcaatcaaa atgtctcagaacgtttacat	Clone THL & KS homologues into Helper1
oJL0240	tggagacttgaccaaacctctggcgaagaagtccaaagcttcatatcttttcaatgacaa	
oJL0241	tcataacctcacgcaaaataacacagtcaaatcaatcaaa atgggtaagggtgaatcgaa	
oJL0242	tggagacttgaccaaacctctggcgaagaagtccaaagctctattctttaataaagatgg	
oJL0243	tcataacctcacgcaaaataacacagtcaaatcaatcaaa atgaaaaattgtgtcatcgt	
oJL0244	tggagacttgaccaaacctctggcgaagaagtccaaagctttaattcaaccgttcaatca	
oJL0245	tcataacctcacgcaaaataacacagtcaaatcaatcaaa atgaaagacgttgtgattgt	
oJL0246	tggagacttgaccaaacctctggcgaagaagtccaaagctctattcgtcacgttcaatgg	
oJL0247	tcataacctcacgcaaaataacacagtcaaatcaatcaaa atggaacaggttgtcattgt	
oJL0248	tggagacttgaccaaacctctggcgaagaagtccaaagctttaaacccgctcaaacaccg	
oJL0363	ttttttagttttaaaacaccagaacttagtttcgacggat atgcctggaaatttatcctt	Clone FOX2 (KR+HTD) homologues from different yeast species into Helper2
oJL0250	ggcgtgaatgtaagcgtgacataactaattacatgatttagttatccaatacaatgacgt	
oJL0365	ttttttagttttaaaacaccagaacttagtttcgacggat atgctttacaaaggcgacac	
oJL0252	gagggcgtgaatgtaagcgtgacataactaattacatgattaagccgttttcaggtcgc	
oJL0367	tttagttttaaaacaccagaacttagtttcgacggatatggaaatgacatcagcgtttac	
oJL0368	gagggcgtgaatgtaagcgtgacataactaattacatgatttattgcaggtcagttgcag	
oJL0369	ttagttttaaaacaccagaacttagtttcgacggatatgtctgagagattgctgttcaag	
oJL0370	agggcgtgaatgtaagcgtgacataactaattacatgatttagttgtctaagactacgac	
oJL0371	tagttttaaaacaccagaacttagtttcgacggatatggggaaagatttgagttttaatg	
oJL0372	gtgaatgtaagcgtgacataactaattacatgatttaattatctagaacaatcttttag	
oJL0373	ttttttagttttaaaacaccagaacttagtttcgacggatatgtcgtcttcaaatctatc	

oJL0374	agggcgtgaatgtaagcgtgacataactaattacatgatttaattatctaaaacaacttg	
oJL0375	ttttagttttaaaacaccagaacttagtttcgacggatatgagtgaattatcatttaaag	
oJL0376	gagggcgtgaatgtaagcgtgacataactaattacatgatttagtccaaaacaatgacac	
oJL0377	ttttttagttttaaaacaccagaacttagtttcgacggatatgagctcacaacaattatc	
oJL0378	gtgaatgtaagcgtgacataactaattacatgatttaattttctaagacaattttatttc	
oJL0379	tttttagttttaaaacaccagaacttagtttcgacggatatgtcgttagaatttaaggac	
oJL0380	gagggcgtgaatgtaagcgtgacataactaattacatgatttagtccaatacgatcttac	
oJL0381	gttttaaaacaccagaacttagtttcgacggatatgacagatactgatttgttatttaag	
oJL0382	gagggcgtgaatgtaagcgtgacataactaattacatgatttaattgtccaaaaccacag	
oJL0383	ttttttagttttaaaacaccagaacttagtttcgacggatatgggtgacaacaagctgag	
oJL0384	gggcgtgaatgtaagcgtgacataactaattacatgatttaattatcaaggacgacatag	
oJL0385	ttttagttttaaaacaccagaacttagtttcgacggatatgtcaggattatccttcaaag	
oJL0386	gagggcgtgaatgtaagcgtgacataactaattacatgatttaattatccaatacaacag	
oJL0387	tttttagttttaaaacaccagaacttagtttcgacggatatgtcgctaactttcaacgac	
oJL0388	gcgtgaatgtaagcgtgacataactaattacatgatttagttggtcaacacaggcatatc	
oJL0389	tttttagttttaaaacaccagaacttagtttcgacggatatgtcccaattaagatttgac	
oJL0390	agggcgtgaatgtaagcgtgacataactaattacatgatttagttactaatgaccacgac	
oJL0391	ttttagttttaaaacaccagaacttagtttcgacggatatgagtgaaatatcattcaaag	
oJL0392	gagggcgtgaatgtaagcgtgacataactaattacatgatttaattattgatggccaatg	
oJL0393	ttttagttttaaaacaccagaacttagtttcgacggatatgggtgagatagagctaaaag	
oJL0394	gggcgtgaatgtaagcgtgacataactaattacatgatttaacggtcaatcaccaaacag	
oJL0395	ttttagttttaaaacaccagaacttagtttcgacggatatgtcagaaatatcatttaaag	
oJL0396	gggcgtgaatgtaagcgtgacataactaattacatgatttagttgttaattgcaatagtc	
oJL0397	ttttagttttaaaacaccagaacttagtttcgacggatatgtcacaattggattttaaag	
oJL0398	gagggcgtgaatgtaagcgtgacataactaattacatgatttaattgttaatagcaatag	
oJL0399	tttttagttttaaaacaccagaacttagtttcgacggatatggatgtactgcagaatag	
oJL0400	gagggcgtgaatgtaagcgtgacataactaattacatgatttagttgttgattgcaatag	
oJL0401	ttttagttttaaaacaccagaacttagtttcgacggatatgtctccaatagatttcaaag	
oJL0402	gagggcgtgaatgtaagcgtgacataactaattacatgatttaattgttaatagcaatag	
oJL0403	ttttagttttaaaacaccagaacttagtttcgacggatatgtctccagttgattttaaag	
oJL0404	gagggcgtgaatgtaagcgtgacataactaattacatgatttagttgttaatggcaatag	
oJL0405	ttttagttttaaaacaccagaacttagtttcgacggatatgtctctattatcctttaaag	
oJL0406	gagggcgtgaatgtaagcgtgacataactaattacatgatttagttgttgatagcgatgg	
oJL0407	ttttagttttaaaacaccagaacttagtttcgacggatatggccccaataagtttcaaag	
oJL0408	gagggcgtgaatgtaagcgtgacataactaattacatgatttaattgttaatagcaatcg	
oJL0409	ttttagttttaaaacaccagaacttagtttcgacggatatgtcggaaatatctttcaaag	
oJL0410	gagggcgtgaatgtaagcgtgacataactaattacatgatttaattgttgatggcaatgg	
oJL0411	tttttagttttaaaacaccagaacttagtttcgacggatatgaaaaaggtagacaacgg	Clone KR homologues from *Yarrowia lipolytica* into Helper2
oJL0412	gagggcgtgaatgtaagcgtgacataactaattacatgattcacatgtatgtccccttg	
oJL0413	tttttagttttaaaacaccagaacttagtttcgacggatatgaagaaggtcgactctctctc	
oJL0414	gagggcgtgaatgtaagcgtgacataactaattacatgatttagtagtcatagaagccc	
oJL0415	tttttagttttaaaacaccagaacttagtttcgacggatatggaaaccaagttgaatgg	
oJL0416	gagggcgtgaatgtaagcgtgacataactaattacatgatctataccgcagacaagccc	
oJL0417	tttttagttttaaaacaccagaacttagtttcgacggatatgtctggagaactaagatac	
oJL0418	ctcccttggaaacaatctcgtcgacgacaacatcggcaactcgcttgccactgccagcc	
oJL0419	cttcaagggcgacggtgcccaggctggcagtggcaagcgagttgccgatgttgtcgtcgac	
oJL0420	gagggcgtgaatgtaagcgtgacataactaattacatgatttaattgctgatggcggtag	

oJL0425	aaggaagtaattatctacttttacaacaaatataaaacaatgcctctcgattactccgc	Clone HTD homologues from *Yarrowia lipolytica* into Helper6
oJL0426	aattagagcgtgatcatgaattaataaaagtgttcgcaaatcacaacttctcgtaagtag	
oJL0427	aaggaagtaattatctacttttacaacaaatataaaacaatgctccgaaccatccgatc	
oJL0428	aattagagcgtgatcatgaattaataaaagtgttcgcaaattactcgttcttgaagttgg	
oJL0429	aaggaagtaattatctacttttacaacaaatataaaacaatgtcacagaccacggcggc	
oJL0430	aattagagcgtgatcatgaattaataaaagtgttcgcaaactagttaacccagtcaagaac	
oJL0431	aaggaagtaattatctacttttacaacaaatataaaacaatgtctttgctgcagaccttcc	
oJL0432	aattagagcgtgatcatgaattaataaaagtgttcgcaaactaaagcttggccttgatctc	
oJL0433	aaggaagtaattatctacttttacaacaaatataaaacaatgggagagacgttcactctg	
oJL0434	aattagagcgtgatcatgaattaataaaagtgttcgcaaattatcgacccttgaaaatgg	
oJL0435	aaggaagtaattatctacttttacaacaaatataaaacaatgcctgccgaacgaacactc	
oJL0436	aattagagcgtgatcatgaattaataaaagtgttcgcaaattactggtggtctctagcag	
oJL0261	tcataacaccaagcaactaatactataacatacaataata atgtcgtcctcagctcatca	Clone TER homologues into Helper3
oJL0262	aaagaaaaaaattgatctatcgatttcaattcaattcaatttaccattctaaaacaacca	
oJL0263	tcataacaccaagcaactaatactataacatacaataata atgaaatgtactataccaga	
oJL0264	aaagaaaaaaattgatctatcgatttcaattcaattcaatctattgtggtatttcaagaa	
oJL0265	tcataacaccaagcaactaatactataacatacaataata atgaatacagcaaacacttt	
oJL0266	gaaaaaaattgatctatcgatttcaattcaattcaatttaatacaactcatgtccaaaat	
oJL0267	tcataacaccaagcaactaatactataacatacaataata atgtccgcctcgattccaga	
oJL0268	aaagaaaaaaattgatctatcgatttcaattcaattcaatttatttcaagacggcaacca	
oJL0269	tcataacaccaagcaactaatactataacatacaataata atgcaagttgcaattccaga	
oJL0270	aaagaaaaaaattgatctatcgatttcaattcaattcaatctagtttaatacggcaacga	
oJL0271	tcataacaccaagcaactaatactataacatacaataata atgaaggctgtcgtcattga	
oJL0272	aaagaaaaaaattgatctatcgatttcaattcaattcaatctagtttaatacggcaacta	
oJL0273	tcataacaccaagcaactaatactataacatacaataata atggatttttctttaactga	
oJL0274	aaagaaaaaaattgatctatcgatttcaattcaattcaatttatttgttctgatagtctt	
oJL0275	tcataacaccaagcaactaatactataacatacaataataatgggttttctttccggtaa	
oJL0276	aaagaaaaaaattgatctatcgatttcaattcaattcaatttatttcagttcgagttcgt	
oJL0277	tcataacaccaagcaactaatactataacatacaataata atggccatgttcaccactac	
oJL0278	aaagaaaaaaattgatctatcgatttcaattcaattcaatttactgctgagctgcgctcg	
oJL0279	taacaccaagcaactaatactataacatacaataataatgattgtaaaaccaatggttag	
oJL0280	aagaaaaaaattgatctatcgatttcaattcaattcaatttaaatcctgtcgaacctttc	
oJL0305	ttaaatctataactacaaaaaacacatacataaactaaaa atgaatcaacaggatattga	Clone EcEutE into Helper4
oJL0306	aaagaaaagaagataatatttttatataattatattaatcttaaacaatgcgaaacgcat	
oJL0557	aaagaaagcatagcaatctaatctaagttttaattacaaaatggttgatttcgaatattc	Clone CaBdhB into Helper5
oJL0558	aaaagatatgcaactagaaaagtcttatcaatctccttacacagatttttgaatatttg	
oJL0537	catcaagaacaaacaagctcaacttgtc	Sequencing primers for genes cloned into Helper plasmids
oJL0538	caagatatcattaaaaatataaaattag	
oJL0539	catatttcttgtcatattcctttctc	
oJL0540	cttttcgtaaatttctggcaaggtag	
oJL0541	cttaacttgtttattattctctcttgtttc	
oJL0542	cttcaggttgtctaactccttcctttttc	
oJL0543	gtatcttttcttcccttgtctcaatc	
oJL0544	ctattattttagcgtaaaggatgggg	
oJL0545	catttactattttcccttcttacg	
oJL0546	caatataaaaaagctttccgtagtcatc	
oJL0547	gtttcatttttcttgttctattacaac	
oJL0548	ccagactatatataaggataaattac	
oJL0549	ggtaggtattgattgtaattctgtaaatc	
oJL0550	ctaattcgtagtttttcaagttcttagatgc	
oJL0551	cctttcttaattctgttgtaattaccttcc	